Johann Wolfgang Goethe-Universität
Frankfurt am Main
Fachbereich Physik
Institut für Theoretische Physik

MASTER THESIS

The Π_u hybrid static potential to $\mathcal{O}(g^2)$ in perturbation theory

Amanda Konieczna

Supervisor
Prof. Dr. Owe PHILIPSEN

Second Supervisor
Prof. Dr. Marc WAGNER

September 24, 2021

Eigenständigkeitserklärung

Erklärung nach § 30 (12) Ordnung für den Bachelor- und den Masterstudiengang

Hiermit erkläre ich, dass ich die Arbeit selbstständig und ohne Benutzung anderer als der angegebenen Quellen und Hilfsmittel verfasst habe. Alle Stellen der Arbeit, die wörtlich oder sinngemäß aus Veröffentlichungen oder aus anderen fremden Texten entnommen wurden, sind von mir als solche kenntlich gemacht worden. Ferner erkläre ich, dass die Arbeit nicht - auch nicht auszugsweise - für eine andere Prüfung verwendet wurde.

Frankfurt am Main, den

_____

(Amanda Konieczna)

Abstract

In this work I investigate the potential of an excited $Q\bar{Q}$ pair in the limit of infinite masses. The hybrid of interest is denoted by quantum numbers Π_u.
The correlation function is calculated by means of perturbation theory, for which I assume small quark-antiquark distances. The excitation is described through an insertion H. It describes a chromoelectric or chromomagnetic field between the quark-antiquark pair. For the case of the Π_u hybrid static potential, on which I focus, the insertion is $H_i = \epsilon_{i3k}(\hat{e}_3)_3 B_k$. I aim to show that the behaviour up to $\mathcal{O}(g^2)$ in perturbation theory equals zero, as predicted by Bali in [1].

Contents

1 Introduction

The Standard Model of particle physics is the currently most accurate description of all fundamental forces except gravity and all known elementary particles.
The interaction of interest for this work is quantum chromodynamics (QCD), the theory of the strong interaction, which was developed in the 1970s. QCD describes the interaction of quarks via the QCD gauge bosons, the gluons. The non-abelian nature of QCD as a SU(3) Yang-Mills theory leads to gluonic self-interactions. This is what makes investigations of the strong interaction especially challenging. QCD accounts for the existence of hadrons, particles consisting of three quarks, as well as mesons consisting of a quark-antiquark pair.
Moreover, so called exotic particles are predicted by QCD. There are several theoretical frameworks which explain how such exotic particles arise. One of the most prominent examples for such a system is the glueball, a particle solely of gluons forming a bound state. In addition, one can predict exotic hadrons within the theory of QCD, see [2][3][4]. An example of those are hybrid mesons, excited systems of a quark and an antiquark. The theory of quantum chromodynamics describes such an excitation by additional gluon fields that lead to higher energy levels and new quantum numbers.

Furthermore, already realised experiments show evidence for the existence of exotic matter. Since 2003 a number of quarkonium-like particles, referred to as XYZ mesons [5], have been discovered. The results seem to fit the theoretical description of hybrid mesons [6].
Such experimental results underline the importance of theoretical investigations into exotic particles. Especially, information on their masses would benefit further experimental search and, hopefully, prove the validity of QCD predictions about exotic hadrons. Upcoming experiments like PANDA at FAIR aim to achieve a deeper understanding of such possible exotic systems.

Theoretical predictions on hybrid meson masses can be made through calculations of their potentials. The masses can be computed when solving a Schrödinger equation that contains the systems ground state potential (see e.g. [7]).
The focus of this work is the calculation of aforementioned hybrid potentials. As widely done within the field, I examine them in the limit of infinite quark masses. Those (anti-)quarks of infinite mass are referred to as *static*. Calculations within the static limit provide a rather good description of heavy hybrid quarkonia like $c\bar{c}$ (charmonium) or $b\bar{b}$ (bottomonium).
One possible investigative method for calculating hybrid static potentials is perturbation theory. This approach is justified by assuming small quark-antiquark separations. It already has been used in order to describe the ordinary static QCD potential as it was done e.g. in [8], [9] or [10].
Within this work I focus on calculating the lowest non-trivial hybrid static potential with quantum numbers Π_u and show, in consistency with a statement made by Bali in [1], that the ground state potential of this system is zero.

2 Theory

In the theoretical part of this work I start with a short reminder of QCD basics and the construction of n-point functions and Feynman diagrams, due to their importance for the actual calculations.
I resume with the introduction of Wilson lines which are necessary for the construction of the Wilson loop and the static potential between an unexcited quark-antiquark pair. Finally, I give a qualitative introduction to hybrid static potentials.
Then, all basics will be provided that are needed for the calculation of the hybrid correlation function.

2.1 The QCD action

The content of this section is fully taken out of [11]. Therefore I omit the citation marks for the rest of this section.

The QCD Lagrangian consists of two major parts: $\mathcal{L}_Q$ which describes quarks, the fermionic elementary particles of QCD and $\mathcal{L}_{YM}$, the contribution of the exchange particles of the strong interaction, the gluons.

The Lagrange function of a quark field is

$$\begin{aligned} \mathcal{L}_Q[\psi,\bar{\psi},\mathcal{A}] = &\sum_f \bar{\psi}_\alpha^{A(f)} \left[i\gamma_{\mu,\alpha\beta}(\delta^{AB}\partial^\mu - ig\mathcal{A}^{\mu,AB}) - \delta^{AB}\delta_{\alpha\beta}m \right] \psi_\beta^{B(f)}, \\ &\text{with} \quad \mathcal{A}^{\mu,AB} = \frac{\lambda^{a,AB}}{2} A^{\mu,a} \quad \text{describing the gluon fields.} \end{aligned} \tag{1}$$

The indices are

- $A, B = 1, ..., 3$ for the fundamental colour index
- $a, b = 1, ..., 8$ for the adjoint colour index
- $\alpha, \beta = 1, ..., 4$ for the Dirac spinor index
- $\mu, \nu = 0, ...3$ for the Lorentz index

In short notation, omitting most of the indices I can also write

$$\mathcal{L}_Q = \sum_f \bar{\psi}_f \left(i\gamma_\mu D^\mu - m \right) \psi_f \tag{2}$$

The exchange particles of QCD are gluons. They guarantee the invariance of quantum chromodynamics under local SU(3) transformations. Therefore their properties can be described in terms of SU(3) Yang-Mills theory with the following Lagrangian:

$$\begin{aligned} \mathcal{L}_{YM} &= -\frac{1}{2}\mathrm{Tr}\left(\mathcal{F}_{\mu\nu}\mathcal{F}^{\mu\nu}\right) \\ &= -\frac{1}{4} F^a_{\mu\nu} F^{\mu\nu,a} \quad \text{with} \quad \mathcal{F}_{\mu\nu} = \frac{\lambda^a}{2} F^a_{\mu\nu} \end{aligned} \tag{3a}$$

where $F_{\mu\nu}$ is the field strength tensor, which is given through

$$F^a_{\mu\nu} = \partial_\mu A^a_\nu - \partial_\nu A^a_\mu + g f^{abc} A^b_\mu A^c_\nu \tag{3b}$$

The gauge fields $\mathcal{A}_\mu = A^a_\mu T^a$ have the form of (3×3)-matrices. The generators T^a of the underlying symmetry group SU(3) are related to the Gell-Mann matrices λ^a via $T^a = \lambda^a/2$. The non-commutative nature of Gell-Mann matrices is the reason behind the self-interaction of gauge fields.
Now the full QCD Lagrangian can be written as

$$\mathcal{L}_{QCD} = \mathcal{L}_Q + \mathcal{L}_{YM} \tag{4}$$

Additionally, when considering QCD one has to deal with so called *Faddeev-Popov ghost fields*. Their role is to eliminate the contributions of redundant, gauge equivalent vector potentials. In non-abelian Yang-Mills theories these Faddeev-Popov ghosts do not decouple from the gauge fields.
They lead to two additional terms in the Lagrangian of QCD, namely

$$\mathcal{L}_{gf} = -\frac{1}{2\xi} \left(\partial_\mu A^\mu\right)^2 \tag{5a}$$

and

$$\mathcal{L}_{FP} = -\bar{\eta}^a \partial_\mu D^{\mu,ab} \eta^b, \quad D^{\mu,ab} = \delta^{ab}\partial^\mu - g f^{abc} A^{\mu,c} \tag{5b}$$

$\mathcal{L}_{gf}$ is the gauge fixing term while $\mathcal{L}_{FP}$ describes the interaction of Faddeev-Popov ghosts with gluons. The choice of the prefactor ξ determines the gauge. The case $\xi = 1$ is called *Feynman gauge*.

2.1.1 Constructing n-point functions for gauge fields

In this work I perform my calculations within the quenched approximation. Therefore I neglect fermion loops when constructing Feynman diagrams. Therefore, when constructing n-point functions I only consider the gluonic contribution.
In general the n-point function G_n of n fields ϕ located at the positions x_1 to x_n can be written as

$$\begin{aligned} G_n(x_1, ..., x_n) &= \langle\Omega| \mathcal{T} \left[\phi(x_1)...\phi(x_n)\right] |\Omega\rangle \\ &= \frac{\langle 0| \mathcal{T} \left[\phi(x_1)...\phi(x_n) S\right] |0\rangle}{\langle 0| S |0\rangle} \end{aligned} \tag{6a}$$

with the scattering matrix S, that describes the transition from initial to final fields and is defined as

$$S = \mathcal{T} \exp\left[-i \int \mathrm{d}^4x \, \mathcal{H}_I(x)\right] \tag{6b}$$

Above, $\mathcal{T}$ is the time-ordering operator and $\mathcal{H}_I$ denotes the interaction part of the theories Hamiltonian. As usually, $|\Omega\rangle$ is the vacuum state of the theory.
The fastest way to evaluate the n-point function is by using Wick's theorem. It states that

$$\langle 0|\,\mathcal{T}\left[\phi(x_1)...\phi(x_n)\right]|0\rangle = \left\{ \begin{array}{c} \text{even } n\text{: sum of all possible Wick contractions} \\ \text{odd } n\text{: } 0 \end{array} \right\} \tag{7a}$$

where a Wick contraction is defined as the expectation value of two fields. Moreover, the contraction generates the Feynman propagator Δ_F, that describes the propagation of a field from one space-time position to another:

$$\langle 0|\,\mathcal{T}\left[\phi(x)\phi(y)\right]|0\rangle = i\Delta_F(x-y) \tag{7b}$$

Making use of Equation 7a requires the S-matrix to be expanded in a power series. Only then one can contract the fields contained in the interaction part of the Hamiltonian.

When dealing with Yang-Mills theory, the Lagrangian in Equation (3a) needs to be expanded, so that the interaction terms, marked by prefactors of g, can be isolated. Then, the S-matrix can be constructed and expanded in a power series.

$$\begin{aligned} \mathcal{L}_{YM} =& -\frac{1}{4}F^a_{\mu\nu}F^{\mu\nu,a} \\ =& -\frac{1}{2}\partial_\mu A^a_\nu\left(\partial^\mu A^{\nu,a} - \partial^\nu A^{\mu,a}\right) \\ & - gf^{abc}\left(\partial^\mu A^{\nu,a}\right)A^b_\mu A^c_\nu \\ & - \frac{g^2}{4}f^{abc}f^{ade}A^b_\mu A^c_\nu A^{\mu,d}A^{\nu,e} \\ \equiv& \mathcal{L}_0 + \mathcal{L}_{I_1} + \mathcal{L}_{I_2} \end{aligned} \tag{8}$$

The calculation shows that there are two possible interactions of gluonic gauge fields. When writing the S-matrix in its best known form, the Dyson series, and inserting the results for the interaction (with $\mathcal{H}_I = \mathcal{H}_{I_1} + \mathcal{H}_{I_2} = \mathcal{L}_{I_1} + \mathcal{L}_{I_2}$) one gets

$$\begin{aligned} S =& \mathcal{T}\exp\left[-i\int_x\left(\mathcal{L}_{I_1}+\mathcal{L}_{I_2}\right)\right] \\ =& \mathcal{T}\left[\exp\left(-i\int_x\mathcal{L}_{I_1}\right)\exp\left(-i\int_x\mathcal{L}_{I_2}\right)\right] \\ =& \sum_{l,m=0}^{\infty}\frac{(-i)^{l+m}}{l!m!}\mathcal{T}\left[\left(\int_x\mathcal{L}_{I_1}\right)^l\left(\int_x\mathcal{L}_{I_2}\right)^m\right] \end{aligned} \tag{9}$$

Now the n-point function

$$G_n(x_1,...,x_n) = \frac{\sum_{l,m=0}^{\infty}\frac{(-i)^{l+m}}{l!m!}\langle 0|\,\mathcal{T}\left[\lambda^{a_1}A_1...\lambda^{a_n}A_n\left(\int_x\mathcal{L}_{I_1}\right)^l\left(\int_x\mathcal{L}_{I_2}\right)^m\right]|0\rangle}{\sum_{l,m=0}^{\infty}\frac{(-i)^{l+m}}{l!m!}\langle 0|\,\mathcal{T}\left[\left(\int_x\mathcal{L}_{I_1}\right)^l\left(\int_x\mathcal{L}_{I_2}\right)^m\right]|0\rangle} \tag{10}$$

describes the interaction of n gluonic fields. Depending on the order to which the S-matrix is expanded, one can calculate the interaction to a certain order in the coupling constant g. Through Wick's theorem (see Eq. (7a)) the fields can be replaced by gluon propagators and the Feynman diagrams can be constructed.

In general the gluon propagator is

$$\Delta^{ab}_{\mu\nu}(x-y) = -\delta^{ab}\int \frac{\mathrm{d}^4k}{(2\pi)^4}\frac{1}{k^2}\left[g_{\mu\nu} + (\xi-1)\,\frac{k_\mu k_\nu}{k^2}\right]e^{-ik(x-y)} \tag{11}$$

I perform my calculations in euclidean space-time using Feynman gauge ($\xi = 1$). In this form the gluon propagator can be written as

$$\bar{\Delta}^{ab}_{\mu\nu}(\bar{x}-\bar{y}) = \delta^{ab}\delta_{\mu\nu}\bar{\Delta}(\bar{x}-\bar{y}) \tag{12a}$$

with

$$\bar{\Delta}(\bar{x}-\bar{y}) = \int \frac{\mathrm{d}^4\bar{k}}{(2\pi)^4}\frac{1}{\bar{k}^2}e^{i\bar{k}(\bar{x}-\bar{y})} \tag{12b}$$

This is the notation I use throughout all calculations.
Now, in contrast to the Minkowski formulation, the propagator is obtained from the gluon fields via

$$\langle 0|\,\mathcal{T}\left[\mathcal{A}^a_\mu(\bar{x})\mathcal{A}^b_\nu(\bar{y})\right]|0\rangle = -\bar{\Delta}^{ab}_{\mu\nu}(\bar{x}-\bar{y}) \tag{13}$$

2.2 The static potential

In a first step it is necessary to introduce the 'ordinary' static potential, before proceeding with the hybrid case.
I start with introducing the *Wilson line*, which is needed in order to construct the static meson state. In the following I use the term $Q\bar{Q}$ in order to describe an infinitely heavy static pair of (anti-)quarks instead of $q\bar{q}$, as I did for ordinary mesons of finite mass.

2.2.1 Wilson lines

In Section 2.1 the invariance of the Lagrangian under local SU(3) transformations had been briefly mentioned. Now I use this property in order to set up the concept of the Wilson line as it was done in [12].
The Dirac spinor field $\psi(x)$ transform in the following way under SU(3) transformations:

$$\psi(x) \to V(x)\psi(x) \quad , \quad V(x) = \exp\left[i\alpha^i(x)\frac{\lambda^i}{2}\right] \tag{14}$$

where α^i are arbitrary functions of x and λ^i are the Gell-Mann matrices, the generators of the SU(3) symmetry group. The Yang-Mills Lagrangian, which is required to be invariant under such transformations, now needs a covariant derivative that is able to compare it at positions x and $x + \epsilon n$, $\epsilon > 0$. Due to the transformation law in Equation (14) a direct comparison is impossible. This problem can be approached by introducing a 4×4 matrix $U(y, x)$ that allows for a comparison of the Dirac fields at positions x and $x + \epsilon n$. This comparator, also known as the *Wilson line*, underlies the transformation law

$$U(y, x) \to V(y)U(y, x)V^\dagger(x) \tag{15}$$

With this definition $U(y, x)\psi(x)$ and $\psi(y)$ have the same transformation properties, which enables the construction of a geometrically meaningful derivative:

$$n^\mu D_\mu \psi(x) = \lim_{\epsilon\to 0} \frac{\psi(x + \epsilon n) - U(x + \epsilon n, x)\psi(x)}{\epsilon} \quad , \quad D_\mu = \partial_\mu - igA^i_\mu \frac{\lambda^i}{2} \tag{16}$$

$\mathcal{A}_\mu = A^i_\mu \frac{\lambda^i}{2}$ is the gauge field that was already introduced in Section (2.1). The most general form of $U(y, x)$ that is valid for arbitrary distances between x and y is

$$U(y, x) = \mathcal{P}\left\{\exp\left[-ig\int_P \mathrm{d}z_\mu \mathcal{A}^\mu(z)\right]\right\} \tag{17}$$

Here P denotes an arbitrary path connecting x and y. The path-ordering operator $\mathcal{P}$ determines the order of Gell-Mann matrices λ in an expansion of the exponential. $U(y, x)$ is a 4×4 tensor in spinor space and a 3×3 tensor in colour space.
The Wilson line has a non-trivial dependence on the chosen path from one space-time point to the other. This can be seen when choosing a closed contour $\mathcal{C}$ as the integration path. In general the expectation value of of such a Wilson line, also known as the *Wilson loop*, is not 1.

$$U(x, x) = \mathcal{P}\left\{\exp\left[-ig\oint_{\mathcal{C}} \mathrm{d}z_\mu \mathcal{A}^\mu(z)\right]\right\} \tag{18}$$

2.2.2 The Wilson loop and the static quark-antiquark potential

The aim of this section is to find a general expression for the potential $V_{Q\bar{Q}}$ of a static quark-antiquark pair.
For a start, the quantity worth consideration is the transition amplitude $K(x_f, x_i)$ of the meson system. In general, the quantum mechanical transition amplitude from a field $\phi(0, \vec{x})$ to $\phi(\bar{t}, \vec{x}')$ can be written as

$$\langle \phi(\bar{t}, \vec{x}') | \phi(0, \vec{x}) \rangle = \sum_{n=0}^{\infty} | \langle \vec{x}' | n \rangle |^2 e^{-(E_n - E_\Omega)\bar{t}} \tag{19}$$

The expression above is given in euclidean spacetime, which is noted by the the bar above the time variable. n are the eigenstates of the theories Hamiltonian to energy eigenvalues E_n, whereas E_Ω denotes the QCD vacuum. Taking the limit of infinite times makes all but the lowest energy difference in the exponent negligible. This results in

$$\lim_{\bar{t}\to\infty} \langle \phi(\bar{t}, \vec{x}') | \phi(0, \vec{x}) \rangle = \lim_{\bar{t}\to\infty} | \langle x' | 0 \rangle |^2 e^{-V_{Q\bar{Q}}\bar{t}} \tag{20}$$

In the equation above I used the definition of the static potential $V_{Q\bar{Q}}$ as the difference between the ground state energy E_0 and the vacuum ($V_{Q\bar{Q}} = E_0 - E_\Omega$).

An analogue expression can also be constructed for a meson system $\Phi(\bar{t})$. Here I define the temporal distance between the initial and the final state to be $\bar{T}$ and the initial positions of quark and antiquark as $x = (0, \vec{x})$ and $y = (0, \vec{y})$; $\vec{x} = \vec{r}/2$ and $\vec{y} = -\vec{r}/2$ with $\vec{r} = (0, 0, r)$.
In the static limit the spatial positions of the (anti-)quarks are not about to change when moving forward in time. Therefore, when assuming $\bar{T}$ to be large, the transition amplitude of the meson system is expected to be

$$\langle \Phi(\bar{T}) | \Phi(0) \rangle \overset{\bar{T}\to\infty}{=} \delta^{(3)}\left(\vec{x} - \vec{x}'\right) \delta^{(3)}\left(\vec{y} - \vec{y}'\right) c_0 e^{-V_{Q\bar{Q}}\bar{T}} \tag{21}$$

The calculation of the static potential $V_{Q\bar{Q}}$ requires another expression for the correlation function $\langle \Phi(\bar{T}) | \Phi(0) \rangle$ to be found. In the following I show, following the calculation in [13], how this correlation function can be written in terms of gluonic gauge fields and a Wilson loop. This allows the calculation of the correlation function in analogy to the n-point function shown in Section 2.1.1.

For constructing the correlation function, first, an expression for the quark-antiquark state $|\Phi\rangle$ is needed.
Quarks and antiquarks are mathematically represented through Dirac fields. As said in Section 2.2.1 two Dirac fields at different space-time positions transform differently under SU(3) transformations unless a gauge link is added to the system. Therefore in order to maintain gauge invariance when constructing a meson, quark and antiquark need to be connected through a Wilson line $U(x, y)$:

$$|\Phi(0)\rangle = \bar{\Psi}^A_\alpha(x) U^{AB}(x, y) \Psi^B_\beta(y) \, |\Omega\rangle \tag{22a}$$

with

$$U(x,y) = \mathcal{P}\left\{\exp\left[ig\int_{-r/2}^{r/2} \mathrm{d}z\, \mathcal{A}_3(z)\right]\right\} \tag{22b}$$

Now the correlation function between the system at time 0 and time T can be easily written as

$$\langle\Phi(T)|\Phi(0)\rangle = -\langle\Omega|\, \Psi^{B'}_{\beta'}(y')U^{A'B'}(y',x')\bar{\Psi}^{A'}_{\alpha'}(x')\bar{\Psi}^{A}_{\alpha}(x)U^{AB}(x,y)\Psi^{B}_{\beta}(y)\,|\Omega\rangle \tag{23}$$

where in the following I insert $x' = (T, \vec{r}/2)$ and $y' = (T, -\vec{r}/2)$.
It can be seen that the expression for the $Q\bar{Q}$ correlation function resembles the equation describing a n-point function in Section 2.1.1 (see Eq. (6a)).
Before the contribution of the gluonic components can be written down in analogy to Eq. (10) and then transformed into Feynman diagrams first the fields of the static (anti-)quarks need to be dealt with. Therefore, in the following I use the path integral representation of the correlation function:

$$\langle\Phi(T)|\Phi(0)\rangle = -\mathrm{Tr}\left[\frac{1}{Z}\int D\Psi D\bar{\Psi}D\bar{\eta}D\eta DA\ \left[\bar{\Psi}^{B'}_{\beta'}(y')...\Psi^{B}_{\beta}(y)\right]\times e^{iS_{QCD}}\right] \tag{24a}$$

where Z is a normalisation constant defined by

$$Z = \int D\Psi D\bar{\Psi}D\bar{\eta}D\eta DA\, e^{iS_{QCD}} \tag{24b}$$

There is a general formula given for integrals of Dirac fields of a similar form to the case above. It can be looked up in Section A.1.3. The exact calculation of static field integrals in the nominator and denominator of Equation (24a) was performed in [13] and can be found in Section A.2.1. The emerging equation for the path integral formulation of the gluonic part of the correlation function can be found in Eq. (103a). When transforming this result back to the bracket formulation and performing a continuation to euclidean space-time the following result emerges:

$$\begin{aligned}\langle\Phi(\bar{T})|\Phi(0)\rangle = &-\delta^{(3)}\left(\vec{x}-\vec{x}'\right)\delta^{(3)}\left(\vec{y}-\vec{y}'\right)\mathrm{Tr}\left[(P_+)_{\alpha\alpha'}(P_-)_{\beta\beta'}\right]e^{-2M\bar{T}} \\ &\times\frac{\langle 0|\,\mathcal{P}\left[e^{-ig\oint_{\mathcal{C}}\mathrm{d}z_\mu\mathcal{A}_\mu(z)}\bar{S}\right]|0\rangle}{\langle 0|\,\bar{S}\,|0\rangle}\end{aligned} \tag{25}$$

The definitions of the prefactors $P_\pm$ can be found in Section A.2.1. $\bar{S}$ denotes the euclidean version of the scattering matrix, which now contains the euclidean action.
This expression can be simplified further more with the definition of the expectation value of the Wilson loop

$$\langle W_{\mathcal{C}}\rangle_{\text{eucl.}} = \frac{\langle 0|\,\mathcal{P}\left[e^{-ig\oint_{\mathcal{C}}\mathrm{d}z_\mu\mathcal{A}_\mu(z)}\bar{S}\right]|0\rangle}{\langle 0|\,\bar{S}\,|0\rangle} \tag{26}$$

where the Wilson line is the rectangular contour in euclidean space-time connecting the points x, x', y' and y.
Now, the final expression for the $Q\bar{Q}$ correlation function becomes

$$\langle \Phi(\bar{T})|\Phi(0)\rangle = -\,\delta^{(3)}\left(\vec{x}-\vec{x}'\right)\delta^{(3)}\left(\vec{y}-\vec{y}'\right)\mathrm{Tr}\left[(P_+)_{\alpha\alpha'}(P_-)_{\beta\beta'}\right]e^{-2M\bar{T}}\,\langle W_{\mathcal{C}}\rangle_{\text{eucl.}} \tag{27}$$

Now I am able to compare both expressions for the correlation function from Equations (21) and (27) and find the following relation between the Wilson loop and the static quark-antiquark potential

$$\langle W_{\mathcal{C}}\rangle_{\text{eucl.}} \overset{\bar{T}\to\infty}{=} \tilde{c_0}e^{(2M-V_{Q\bar{Q}})\bar{T}} \quad , \quad \tilde{c_0} = -\frac{c_0}{\mathrm{Tr}\left[(P_+)_{\alpha\alpha'}(P_-)_{\beta\beta'}\right]} \tag{28a}$$

$$\Rightarrow V_{Q\bar{Q}} = -\lim_{\bar{T}\to\infty}\frac{1}{\bar{T}}\ln\left(\langle W_{\mathcal{C}}\rangle_{\text{eucl.}}\right) \tag{28b}$$

$2M$ is a constant term describing the mass of the pair, what makes it irrelevant to the static potential. Therefore it is abandoned in Equation (28b). The factor $\ln\tilde{c}_0/\bar{T}$ was ejected in the last equation because $\tilde{c}_0$ is a finite factor which makes the term equal to zero in the limit of large temporal loop extensions.

The upper equation is the most typical form to express the static potential in dependence of the Wilson loop. Alternatively one can find another useful formulation when deriving Equation (28a):

$$\begin{aligned}\langle \dot{W}_{\mathcal{C}}\rangle_{\text{eucl.}} \overset{\bar{T}\to\infty}{=} (2M - V_{Q\bar{Q}})\tilde{c_0}e^{(2M-V_{Q\bar{Q}})\bar{T}} &= (2M - V_{Q\bar{Q}})\,\langle W_{\mathcal{C}}\rangle_{\text{eucl.}} \\ \Rightarrow V_{Q\bar{Q}} &= -\,\frac{\langle \dot{W}_{\mathcal{C}}\rangle_{\text{eucl.}}}{\langle W_{\mathcal{C}}\rangle_{\text{eucl.}}}\end{aligned} \tag{29}$$

For the computation of actual masses of the meson system a Schrödinger equation containing the static potential needs to be solved. The resulting energy eigenvalues, that represent the binding energy of the quark-antiquark pair are then used to calculate the masses. For details on this procedure see [7].

2.3 Hybrid static potentials

Inside the quark model the quantum numbers of $q\bar{q}$ meson systems are determined by the particles orbital angular momentum L and and the (anti-)quark spin S. The quantum numbers are (see [14])

- $|L - S| \leq J \leq |L + S|$ which is the systems total angular momentum
- $\mathcal{P} = (-1)^{L+1}$ describing the systems properties under parity transformations: $(t, \vec{r}) \rightarrow (t, -\vec{r})$
- $\mathcal{C} = (-1)^{L+S}$, the behaviour of the system under charge conjugation.

Still, as already mentioned in Section 1, there is experimental evidence for the existence of systems with quantum numbers other than the ones predicted by the constituent quark model. One example are the $J^{\mathcal{PC}} = 1^{-+}$ states $\pi_1(1400)$ and $\pi_1(1400)$ [15]. Such particles were therefore considered as 'exotic' (see [16]).
The introduction of hybrid mesons delivers a possible explanation for the existence of these quantum numbers [15]. In this approach, excited gluon fields contribute to the overall quantum numbers of the $q\bar{q}$-system.

Hybrid quantum numbers

The classification of hybrid mesons in the static limit ($m \rightarrow \infty$) is based on their behaviour under symmetry transformations. The according symmetry group is $D_{\infty h}$ [17], the infinite dihedral point group which is also used to describe diatomic molecules [18]. Quantum numbers of hybrid static potential $\Lambda_\eta^{\sigma_v}$ are given as [19]

- $\Lambda = 0, 1, 2, ... = \Sigma, \Pi, \Delta, ...$ the total angular momentum of the system
- $\eta = u, g$ denoting the systems behaviour under a combination of parity transformation and charge conjugation: $\mathcal{P} \circ \mathcal{C}$
- $\sigma_v = \pm 1$ giving the systems transformation property under a reflection along an axis which is perpendicular to the $Q\bar{Q}$ separation axis.

Note that Λ equals the angular momentum of the gluonic excitation. Since I work in the infinite mass limit, there are no contributions of individual spins. Moreover, σ_v only contributes to the quantum numbers when $\Lambda = 0$, due to its degeneracy for higher angular momenta.

Insertions

In Equation (22a) static meson systems were written in terms of quantum mechanical states. When considering hybrids an additional field operator $\hat{H}$ needs to be implemented as a source of the additional gluonic excitation. It is located on the Wilson line connecting the quark fields Ψ and $\bar{\Psi}$. This field operator is referred to as an *insertion*. It consists of a chromoelectric or chromomagnetic field, whose choice depends on the quantum numbers which one wants to construct.
Here is a short overview over the different hybrid quantum numbers and the according field operators:

$\Lambda_\eta^{\sigma_v}$	$\hat{H}^a$
Σ_g^-	$(\hat{r}\cdot\vec{D})(\hat{r}\cdot\vec{B})$
Σ_u^+	$(\hat{r}\cdot\vec{D})(\hat{r}\cdot\vec{E})$
Σ_u^-	$\hat{r}\cdot\vec{B}$
Π_u	$\hat{r}\times\vec{B}$
Π_g	$\hat{r}\times\vec{E}$
Δ_u	$(\hat{r}\times\vec{D})^i(\hat{r}\times\vec{E})^j+(\hat{r}\times\vec{D})^j(\hat{r}\times\vec{E})^i$
Δ_g	$(\hat{r}\times\vec{D})^i(\hat{r}\times\vec{B})^j+(\hat{r}\times\vec{D})^j(\hat{r}\times\vec{B})^i$

Table 1: Examples for gluonic excitation operators for hybrid static potentials of different quantum numbers

The table was taken from [20]. The Σ_g^+ hybrid was not included since it corresponds only to the ground state potential. The unit vector $\hat{r}$ points along the direction of the $Q\bar{Q}$ axis, which usually is the z-axis.

3 Perturbative expansion of the hybrid Wilson loop

In Section 2.2.2 a formula for the static potential of an ordinary quark-antiquark pair in euclidean space-time has been derived. All following calculations are formulated in euclidean notation, though now I omit the bars denoting euclidean times and frequencies.

In order to construct excited systems, the state $|\Phi(x)\rangle$ needs to be extended by a term that describes the excitation. This is done by locating an insertion on an axis of the Wilson loop. In my calculation the insertion is positioned at $y = (-T/2, \vec{0})$ and $y' = (T/2, \vec{0})$, the midpoints of the spatial axes that connect quark and antiquark.
In all of the following calculations the positions of the loop corners are $x_1 = (-T/2, \vec{r}/2)$, $x_2 = (-T/2, -\vec{r}/2)$, $x_1' = (T/2, \vec{r}/2)$ and $x_2' = (T/2, -\vec{r}/2)$. The temporal positions of the quarks are shifted by $-T/2$ due to symmetry reasons.

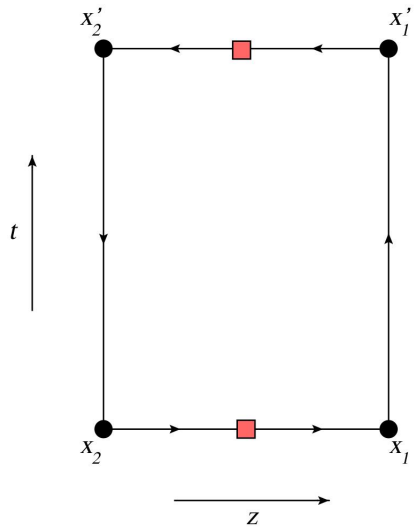

The insertion $\hat{H} = H_\mu^{AB}$ is an operator with one Lorentz index and two fundamental colour indices A and B. Including this operator into the state $|\Phi(-T/2)\rangle$ results in

$$|\Phi(-T/2)\rangle = \bar{\Psi}_\alpha^A(x_1)\gamma_5 U^{AA'}(x_1, 0) H^{A'B'} U^{B'B}(0, x_2)\Psi_\beta^B(x_2)\,|\Omega\rangle \tag{30}$$

When integrating out the static quark fields in analogy to the procedure in Section 2.2.2, I get the following result for the correlation function

$$\begin{aligned} &\langle\Phi(T/2)|\Phi(-T/2)\rangle \\ &= -\,\delta^{(3)}\left(\vec{x}_1 - \vec{x}_1'\right)\delta^{(3)}\left(\vec{x}_2 - \vec{x}_2'\right)\mathrm{Tr}\left[(P_+)_{\alpha\alpha'}(P_-)_{\beta\beta'}\right] e^{-2MT}\,\langle W_\mathcal{C}\rangle_{\text{eucl.}} \end{aligned} \tag{31}$$

In the hybrid case only the Wilson loop expectation value differs from the result in Section 2.2.2. Here the $\hat{H}$ operators need to be added to the expression. Then the Wilson loop becomes

$$\langle W_\mathcal{C}\rangle_{\text{eucl.}} = \frac{\langle 0|\,\mathcal{P}\left[H_\mu^{AB}(-T/2, \vec{0}) H_\nu^{AB}(T/2, \vec{0}) e^{-ig\oint_\mathcal{C} \mathrm{d}z_\mu \mathcal{A}_\mu(z)} S\right]|0\rangle}{\langle 0|\,S\,|0\rangle} \tag{32}$$

The contribution

$$C(A) = H_\mu^{AB}(-T/2,\vec{0})H_\nu^{AB}(T/2,\vec{0})e^{-ig\oint_C \mathrm{d}z_\mu \mathcal{A}_\mu(z)} \tag{33}$$

generates the gluon fields on the loop contour.
In all the following chapters $C(A)$ denotes the currently needed set of fields generated on the loop contour. They all contribute to the total number of different field combinations that emerge when expanding Equation (33) as a sum with respect to orders of g. In the following $C(A)$ is called the *contour field generator*.

The insertion $\hat{H}$ is always proportional to space-time components of the QCD field strength tensor. Therefore for every possible order of g, even g^0, it is inevitable to have gluon lines emerging from the insertions positions. Still other gluon field lines can be generated on the loop contour when expanding the exponential $\exp\left[-ig\oint_C \mathrm{d}z_\mu \mathcal{A}_\mu(z)\right]$.

My goal is to determine the Wilson loop, which is given in Equation (32), up to the second order in g. This allows me to draw conclusions on the hybrid static potential due to the relation from Equation (28b).
The perturbative order of a diagram is determined by the number and order of vertices, as well as the gluon fields that are generated on the contour. Therefore, it is necessary to expand Equation (33) to $\mathcal{O}(g^2)$. Then, making use of the Feynman rules, for each order of the expansion, the gauge fields are connected through gluon propagators and loops in all possible ways.
Working in the quenched approximation allows me to ignore the contributions of fermion loops. Moreover, up to the second order in g there is only one possible diagram that involves ghost fields, though it does not contribute to the potential due to its r-independence.

Adding the vertices of course contributes to the order of the diagram and only diagrams that in total don't exceed the order g^2 are constructed.

3.1 Loop expansion

The expansion of $\exp\left[-ig\oint_C \mathrm{d}z_\mu \mathcal{A}_\mu(z)\right]$ can be performed immediately and is independent of the insertion. In general the expansion of a Wilson line

$$U(x,y) = \mathcal{P}\left\{ \exp\left[\frac{ig}{2}\int_x^y \mathrm{d}z_\mu A_\mu^a(z)\lambda^a\right]\right\} \tag{34}$$

can be expressed as

$$\begin{aligned} U(x,y) &= \mathbb{1} + \frac{ig}{2}\int_0^1 \mathrm{d}\lambda \frac{\mathrm{d}z_\mu(\lambda)}{\mathrm{d}\lambda} A_\mu^a(z(\lambda))\lambda^a \\ &- \frac{g^2}{8}\int_0^1 \mathrm{d}\lambda\mathrm{d}\tau \frac{\mathrm{d}z_\mu}{\mathrm{d}\lambda}\frac{\mathrm{d}z_\nu}{\mathrm{d}\tau} A_\mu^a(z(\lambda))A_\nu^b(z(\tau))\left[\lambda^a\lambda^b\theta(\lambda-\tau)+\lambda^b\lambda^a\theta(\tau-\lambda)\right] \\ &+ \mathcal{O}(g^3) \end{aligned} \tag{35}$$

The expansion only needs to be performed up to the second order since this is the order of interest for my calculations.

In order to simplify the calculation the tensor field $\mathcal{A}_\mu$ is decomposed into $A^a_\mu \lambda^a/2$. Then the path ordering applies only to the Gell-Mann matrices while the gluon field components can now be moved freely.
Due to the insertions that part the spatial lines of the loop in half, there are six loop sections that need to be expanded: the two temporal axes and four sections on the spatial axes. The Wilson line sections are

$$U(z,y) = \mathcal{P}\left\{ \exp\left[\frac{ig}{2} \int_{-r/2}^{0} \mathrm{d}s \; A_3^a(-T/2, \vec{s})\lambda^a \right] \right\} \tag{36a}$$

$$U(x,z) = \mathcal{P}\left\{ \exp\left[\frac{ig}{2} \int_{0}^{r/2} \mathrm{d}s \; A_3^a(-T/2, \vec{s})\lambda^a \right] \right\} \tag{36b}$$

$$U(x',x) = \mathcal{P}\left\{ \exp\left[\frac{ig}{2} \int_{-T/2}^{T/2} \mathrm{d}t \; A_0^a(t, \vec{r}/2)\lambda^a \right] \right\} \tag{36c}$$

$$U(z',x') = \mathcal{P}\left\{ \exp\left[\frac{ig}{2} \int_{r/2}^{0} \mathrm{d}s \; A_3^a(T/2, \vec{s})\lambda^a \right] \right\} \tag{36d}$$

$$U(y',z') = \mathcal{P}\left\{ \exp\left[\frac{ig}{2} \int_{0}^{-r/2} \mathrm{d}s \; A_3^a(T/2, \vec{s})\lambda^a \right] \right\} \tag{36e}$$

and

$$U(y,y') = \mathcal{P}\left\{ \exp\left[\frac{ig}{2} \int_{T/2}^{-T/2} \mathrm{d}t \; A_0^a(t, -\vec{r}/2)\lambda^a \right] \right\} \tag{36f}$$

that are connected into the loop via

$$U(y,y')U(y',z')\lambda^a U(z',x')U(x',x)U(x,z)\lambda^{a'}U(z,y) \tag{37}$$

Note that in between each two spatial sections I added another Gell-Mann matrix. This two matrices originate from the insertions that divide the spatial Wilson lines. Due to path ordering this matrices are fixed in this positions and cannot be ignored. The details of their origin are discussed in the following section.

3.2 Insertion for Π_u potential

For the hybrid static potential of quantum numbers Π_u the insertion consists of a chromomagnetic field $B_i^a = -\epsilon_{ijk}F^{jk,a}/2$ pointing in a direction orthogonal to the spatial lines of the loop. Choosing them to be aligned along the x_3 axis the insertion is

$$H_i^{AB} = \epsilon_{i3k}(\hat{e_3})_3 B_k^{AB} \;,\; B^{AB} = B^a \lambda^{a,AB}/2 \tag{38}$$

Using the relation between B and the field strength tensor $\epsilon_{ijk}B_i^{AB} = -\mathcal{F}_{jk}^{AB}$ the full expression for the insertion Π_u becomes

$$\begin{aligned} H_i =& -\mathcal{F}_{i3} \\ =& -\left(\partial_i \mathcal{A}_3 - \partial_3 \mathcal{A}_i - ig\left[\mathcal{A}_i, \mathcal{A}_3\right]\right) \\ =& -\frac{\lambda^a}{2}\left[\partial_i A_3^a - \partial_3 A_i^a + g f^{abc} A_i^b A_3^c\right] \end{aligned} \tag{39}$$

Note that again the decomposition of $\mathcal{A}_\mu$ into $A_\mu^a \lambda^a/2$ was made.
This equation shows how an insertion can contribute to the gluon fields on the loop contour. It can either contribute with one field of the form $\partial_\mu A_\nu$ in which case there are no orders of g added to the diagram or with $g f^{abc} A_\mu^b A_\nu^c$ where two gluon fields are generated at the insertion and a factor of g is added. The first kind of contribution is called Type I and the latter one Type II.
Now, starting with the general expression for one insertion in Eq. (39) I construct the equation for the contribution of both insertions to the contour field generator:

$$\begin{aligned} &\left[\partial_i A_3^a(y) - \partial_3 A_i^a(y) + g f^{abc} A_i^b(y) A_3^c(y)\right] \\ &\times \left[\partial_i A_3^{a'}(y') - \partial_3 A_i^{a'}(y') + g f^{a'b'c'} A_i^{b'}(y') A_3^{c'}(y')\right] \\ =&\left[\partial_i A_3^a(y) - \partial_3 A_i^a(y)\right]\left[\partial_i A_3^{a'}(y') - \partial_3 A_i^{a'}(y')\right] \\ &+ g\Big[f^{abc} A_i^b(y) A_3^c(y)\left(\partial_i A_3^{a'}(y') - \partial_3 A_i^{a'}(y')\right) \\ &\quad + f^{a'bc} A_i^b(y') A_3^c(y')\Big(\partial_i A_3^a(y) - \partial_3 A_i^a(y)\Big)\Big] \\ &+ g^2 f^{abc} f^{a'b'c'} A_i^b(y) A_3^c(y) A_i^{b'}(y') A_3^{c'}(y') \end{aligned} \tag{40}$$

In summary there are three different cases that show how the insertions can contribute to the contour field generator $C(A)$:

$$\begin{aligned} C(A) =& \frac{\lambda^a \lambda^{a'}}{4}\left[\partial_i A_3^a(y) - \partial_3 A_i^a(y)\right]\left[\partial_i A_3^{a'}(y') - \partial_3 A_i^{a'}(y')\right] e^{-ig\oint_C \mathrm{d}z_\mu A_\mu} \\ =& \frac{\lambda^a \lambda^{a'}}{4}\Big[\partial_i A_3^a(y)\partial_i A_3^{a'}(y') - \partial_i A_3^a(y)\partial_3 A_i^{a'}(y') \\ &- \partial_3 A_i^a(y)\partial_i A_3^{a'}(y') + \partial_3 A_i^a(y)\partial_3 A_i^{a'}(y')\Big] e^{-ig\oint_C \mathrm{d}z_\mu A_\mu} \end{aligned} \tag{41a}$$

$$\begin{aligned} C(A) =& \frac{1}{4} g \lambda^a \lambda^{a'} f^{a'bc}\left[\partial_i A_3^a(y) - \partial_3 A_i^a(y)\right] A_i^b(y') A_3^c(y')\, e^{-ig\oint_C \mathrm{d}z_\mu A^\mu} \\ =& \frac{1}{4} g \lambda^a \lambda^{a'} f^{a'bc}\left[\partial_{y_i} A_3^a(y) A_i^b(y') A_3^c(y') - \partial_{y_3} A_i^a(y) A_i^b(y') A_3^c(y')\right] e^{-ig\oint_C \mathrm{d}z_\mu A_\mu} \end{aligned} \tag{41b}$$

$$C(A) = \frac{1}{4} g^2 \lambda^a \lambda^{a'} f^{abc} f^{a'b'c'} A_i^b(y) A_3^c(y) A_i^{b'}(y') A_3^{c'}(y')\, e^{-ig\oint_C \mathrm{d}z_\mu A_\mu} \tag{41c}$$

The second case can be mirrored with respect to the $t = 0$ axis.

4 Discussion of basic diagrams

Diagrams contributing with $\mathcal{O}(g^2)$ to the hybrid static potentials can consist of products of diagrams with smaller order. In the following I discuss this basic diagrams separately. This makes it possible to immediately draw conclusions for the combined diagrams.
The starting point of all following calculations is Equation (32). From there I pick fitting terms from $C(A)$ (see Eq. (33)) that generates the gluon fields on the loop contour. Since only simple propagators are considered as basic diagrams no vertices or loops enter the calculations in this chapter.

In general diagrams that do not depend on the $Q\bar{Q}$ distance r like e.g. self-energy corrections aren't considered since per definition they do not contribute to the hybrid static potential $V(r)$.

4.1 Propagator between insertions of Type I

First $C(A)$ is to be determined. For the propagator of interest no fields from the Wilson lines contribute, therefore the expansion of the exponential factor $\exp\left[-ig \oint_{\mathcal{C}} \mathrm{d}z_\mu \mathcal{A}_\mu(z)\right]$ only contributes with the term 1.
When both insertions contribute with Type I

$$\partial_i A_3^a - \partial_3 A_i^a \tag{42}$$

in analogy to Equation (41a) the full expression for $C(A)$ becomes

$$\begin{aligned}\frac{\lambda^a\lambda^{a'}}{4}\Big[&\partial_i A_3^a(y)\partial_i A_3^{a'}(y') - \partial_i A_3^a(y)\partial_3 A_i^{a'}(y') \\ &- \partial_3 A_i^a(y)\partial_i A_3^{a'}(y') + \partial_3 A_i^a(y)\partial_3 A_i^{a'}(y')\Big]\end{aligned} \tag{43}$$

Each pair of fields can be contracted with Wick's theorem into a propagator. The combination $A_i A_3 \to \Delta_{i3} = \delta_{i3}\Delta = 0$ $(i = 1, 2)$ vanishes immediately due to unmatching Lorentz indices. When ignoring prefactors I get the following result for the remaining part of the diagram:

$$\begin{aligned}&\langle 0|\, \lambda^a\lambda^{a'} \left[\partial_i A_3^a(y)\partial_i A_3^{a'}(y') + \partial_3 A_i^a(y)\partial_3 A_i^{a'}(y')\right] |0\rangle \\ =& -\mathrm{Tr}\left[\lambda^a\lambda^{a'}\left(\partial_{y_i}\partial_{y_i'}\Delta_{33}^{aa'}(y'-y) + \partial_{y_3}\partial_{y_3'}\Delta_{ii}^{aa'}(y'-y)\right)\right] \\ =& -16\left(\partial_{y_i}\partial_{y_i'} + \partial_{y_3}\partial_{y_3'}\right)\Delta(y'-y)\end{aligned} \tag{44}$$

In the last line used $\mathrm{Tr}\left[\lambda^a\lambda^a\right] = 16$ (see Eq. (85)).
When the propagator is written in coordinate space the derivatives can be performed easily:

$$
\begin{aligned}
&\left(\partial_{y_i}\partial_{y_i'} + \partial_{y_3}\partial_{y_3'}\right) \int_k \frac{1}{(2\pi)^4}\frac{1}{k^2} e^{ik(y'-y)} \\
=&\frac{1}{(2\pi)^2}\left(\partial_{y_i}\partial_{y_i'} + \partial_{y_3}\partial_{y_3'}\right)\frac{1}{(y'-y)^2} \\
=&\frac{1}{(2\pi)^2}\left[\left(\frac{2}{(y'-y)^4} - \frac{8(y_i'-y_i)^2}{(y'-y)^6}\right) + \left(\frac{2}{(y'-y)^4} - \frac{8(y_3'-y_3)^2}{(y'-y)^6}\right)\right] \\
=&\frac{4}{(2\pi)^2}\left[\frac{1}{(y'-y)^4} - 2\frac{(y_i'-y_i)^2 + (y_3'-y_3)^2}{(y'-y)^6}\right]
\end{aligned}
\tag{45}
$$

In the first step the propagator was Fourier transformed according to the calculation in Section A.1.4.
Now, since no derivatives are left the definitions $y = (-T/2, \vec{0})$ and $y' = (T/2, \vec{0})$ can be inserted. Then the second term in the expression above vanishes immediately, which reduces the last line of Equation (45) to

$$
\frac{1}{\pi^2 T^4} \tag{46}
$$

Now, I can use the fact that the Wilson loop is regarded in the limit of large temporal extensions T. Then, due to the factor of T^4 in the denominator the propagator becomes zero.

4.2 Propagator between insertion of Type I and insertion of Type II

The diagram discussed in this section is fairly similar to the one discussed above. It differs in one of the two insertions having a Type II contribution to the diagram. There are two equivalent cases to construct this diagram depending on which of them contributes with which Type.
In the following calculation I choose the insertion at z to have a Type I contribution and the upper insertion at z' a Type II contribution.
This results in the following expression for $C(A)$ according to Equation (41b):

$$
g\frac{\lambda^a\lambda^{a'}}{4} f^{a'bc}\left[\partial_{y_i} A_3^a(y) A_i^b(y') A_3^c(y') - \partial_{y_3} A_i^a(y) A_i^b(y') A_3^c(y')\right] \tag{47}
$$

Since the fields on both ends of a propagator need to have the same Lorentz index in each term there is only one possible way to connect two of three fields through a propagator. It needs to be kept in mind that a resulting diagram needs to have some more components in order to bind the remaining field.
Still, at this point my only interest is the behaviour of the propagator connecting the insertions. The two versions of this propagator that can be constructed are $\Delta_{33}^{ac}(y'-y)$ and $\Delta_{ii}^{ab}(y'-y)$. As can be seen in Equation (47), each version has an attached derivative that originates in the

Type I insertion. When deriving the propagators I get

$$\begin{aligned}\partial_{y_i}\Delta_{33}^{ac}(y'-y) =&\partial_{y_i}\int_k \frac{1}{(2\pi)^4}\frac{1}{k^2}e^{ik(y'-y)}\\ =&\frac{1}{(2\pi)^2}\partial_{y_i}\frac{1}{(y'-y)^2}\\ =&-\frac{2}{(2\pi)^2}\frac{y_i'-y_i}{(y'-y)^4}\\ =&-\frac{1}{2\pi^2}\frac{0}{(y'-y)^4}\\ =&0\end{aligned} \tag{48a}$$

and analogously

$$\begin{aligned}\partial_{y_3}\Delta_{ii}^{ab}(y'-y) =&\frac{1}{2\pi^2}\frac{y_3'-y_3}{(y'-y)^4}\\ =&\frac{1}{2\pi^2}\frac{0}{(y'-y)^4}\\ =&0\end{aligned} \tag{48b}$$

The propagators become trivially zero due to vanishing nominators, since $\vec{y}=\vec{y}'=\vec{0}$.

4.3 Propagator between two fields at one insertion

To investigate this propagator one only needs to take into consideration one of the insertions contributing with Type II to an otherwise arbitrary diagram. Both fields that are generated at this position are connected into a propagator:

$$\begin{aligned}\langle 0|\,\lambda^a f^{abc}A_i^b(y)A_3^c(y)\,|0\rangle =&-\operatorname{Tr}\left[\lambda^a f^{abc}\Delta_{i3}^{bc}(0)\right]\\ =&-\operatorname{Tr}\left[\lambda^a f^{abc}\delta^{bc}\delta_{i3}\Delta(0)\right]\\ =&-\operatorname{Tr}\left[\lambda^a f^{abb}\right]\delta_{i3}\Delta(0)=0\end{aligned} \tag{49}$$

No propagator that connects gluon fields generated at a Type II contribution of an insertion can exist. Both the structure constant f^{abb} and δ_{i3} become zero.

4.4 Propagator between insertion of Type I and spatial axis

In this case the contour field generator $C(A)$ has the following form

$$C(A) = -ig\frac{\lambda^a\lambda^b}{4}\left[\partial_i A_3^a(y) - \partial_3 A_i^a(y)\right]\int \mathrm{d}z_3\; A_3^b(z)\; H_i(y') \tag{50}$$

Here I chose to connect the y insertion to the spatial axis. The insertion located at y' still has some contribution of Type I or II to the diagram but is left arbitrary, since it is of no interest for the problem at hand.
Note that due to the ordering of the Gell-Mann matrices the upper equation only applies for the case where the contribution of the spatial axis is on the right hand side of the loop. Still, apart of that difference the other case would work completely analogous.
From Equation (50) it is immediately clear, that a propagator can only be constructed between the fields $A_3^a(y)$ and $A_3^b(z)$. Otherwise the Kronecker delta would make the expression vanish ($\delta_{i3} = 0$).
The diagram becomes

$$\langle 0|\,\lambda^a\lambda^b\partial_{y_i}A_3^a(y)A_3^b(z)\,|0\rangle = -\mathrm{Tr}\left[\lambda^a\lambda^b\partial_{y_i}\Delta_{33}^{ab}(z-y)\right] = -16\;\partial_{y_i}\Delta(z-y) \tag{51}$$

For the case where $y_0 = -T/2$ I get

$$\begin{aligned}\partial_{y_i}\Delta(z-y) =& \partial_{y_i}\int_k \frac{1}{(2\pi)^4}\frac{1}{k^2}e^{ik(z-y)}\\ =& \frac{1}{(2\pi)^2}\partial_{y_i}\frac{1}{(z-y)^2}\\ =& -\frac{2}{(2\pi)^2}\frac{z_i-y_i}{(z-y)^4}\\ =& 0\end{aligned} \tag{52}$$

The result for the propagator is zero due to $y_i = z_i = 0$. The same would happen when choosing the insertion at y' due to $y_i = y_i' = 0$. Also the choice $z_0 = +T/2$ would not alter this result.
It is worth noting that the field generated on the spatial axis could also arise from the expansion of the Wilson line exponential $\exp\left[\frac{ig}{2}\int \mathrm{d}z_3\; A_3^b(z)\lambda^b\right]$ to a higher order. Then, according to Equation (35) an additional number of integrations over the axis would arise, as well as Heaviside functions that do not apply to the simple first order case in Equation (50). Though, after closer consideration one can see, that this doesn't alter the result found above, since the propagators vanish all for themselves, independently any other possible terms.

5 Order $\mathcal{O}(g^0)$

There is exactly one diagram that can be built in the zeroth order of the coupling constant. Regarding Equation (33) it can be seen that only the contour field generator $C(A)$ can add to the expression with insertions of Type I. No propagators can be attached to the loop since every field on the contour would add a factor of g. Therefore the expansion of the Wilson loop exponential contributes with its zeroth order.
The only diagram in the zeroth order of g is the one discussed in Section 4.1. Its discussion showed that $\mathcal{O}(g^0)$ does not contribute to the hybrid static potential.

6 Odd orders of g: $\mathcal{O}(g^{2n+1})$

It is possible to show that in general no contributions to the potential can arise from odd orders in the expansion of the Wilson loop with respect to g.

The total order g^n of a diagram consists of the contributions that arise from the external gauge fields located at the contour of the loop g^{n_c} and the orders of g that arise from the vertices connecting the external fields, g^{n_v}. I can write $n = n_c + n_v$.

In my approach n_c is chosen freely and from there I draw conclusions on how many orders n_v of g emerge when connecting the contour fields into vertices.
First I need to find the number of fields generated on the contour when starting with a certain value of n_c.
Equation (35) shows that each external field generated at a Wilson line has exactly one order of g attached.
To take into account the contribution of the insertion Equation (39) needs to be taken into account. It shows that the insertion generates a gauge field with no factor of g attached to it in any case. Moreover, due to the g-dependent term $gf^{abc}A_i^b A_3^c$ one can obtain an additional gauge field, this time with one order of g.
One can conclude, when considering both insertions, that the total number of external fields is $2 + n_c$.

What remains is to conclude, how many orders n_v of g result from a certain number of external fields. A diagram with a odd order of g from its vertices can also only have an odd number of legs. On the other hand a diagram with an even n_v from its vertices can only have an even number of legs. Therefore, I get $n_v = [(2 + n_c) \bmod 2] + 2m,\ m \in \mathbb{N}$.
This result leads me to the following conclusion on the possible orders of diagrams constructed on a Wilson loop:

$$n = n_c + n_v = n_c + (n_c \bmod 2) + 2m \tag{53}$$

where I made use of the relation $(a + nb) \bmod b = a \bmod b$. Analysing Equation (53) one sees that $n_c + (n_c \bmod 2)$ always results in an even number. Therefore, I conclude that only even orders in the expansion of the correlation function can exist.

7 Order $\mathcal{O}(g^2)$

When getting to $\mathcal{O}(g^2)$ the number of possible diagrams gets considerably bigger, what makes it necessary to get some structure into them. I sort them with respect to the origins of the g factors contributing to the given order. A distinction is made between factors of the coupling constant g originating at vertices (n_v) and the contour ($n_c = n_i + n_w$) that can be divided further into a contribution from the insertions (n_i) and the Wilson lines (n_w). The types of diagrams resulting from that consideration can be summarised in a table:

	$n_c = 2$			$n_c = 1$		$n_c = 0$
	$n_i = 2$ $n_w = 0$	$n_i = 1$ $n_w = 1$	$n_i = 0$ $n_w = 1$	$n_i = 1$ $n_w = 0$	$n_i = 0$ $n_w = 1$	$n_i = 0$ $n_w = 0$
$n_v = 0$	v0.c2.2	v0.c2.1	v0.c2.0			
$n_v = 1$				v1.c1.1	v1.c1.0	
$n_v = 2$						v2.c0.0

Table 2: The table shows how the different possible diagrams are organised into groups. The expressions $v0$, $v1$ and $v2$ set the number of orders of g from the vertices in a diagram. $c0$, $c1$ and $c2$ set how many orders of g are generated on the loop contour (loop *and* insertions). For the investigation of $\mathcal{O}(g^2)$ the sum of both numbers of course must be two. The last number finally defines how many orders of g on the contour come from the insertions.

In the following all possible diagrams that can contribute to $\mathcal{O}(g^2)$ of the potential are listed step by step.

v2.c0.0

Considering the Feynman rules there are two possible diagrams that connect gauge fields of Type I on the insertions through a vertex of order g^2. They are

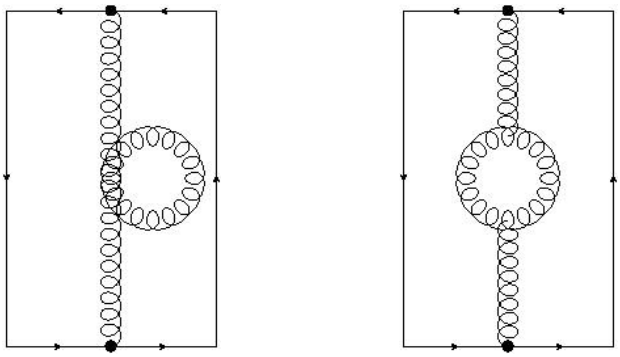

(a) (b)

Figure 1

The diagram depicted in Fig. (1b) could also have a ghost loop in between the two gluon fields that are attached to the lower and upper insertion.

Still, as said at the beginning of Section 4 the contribution of diagrams with no r-dependence to the potential can be neglected. Therefore there is no need for a further investigation of this two diagrams.

v1.c1.0

The diagrams that can be constructed in this section are

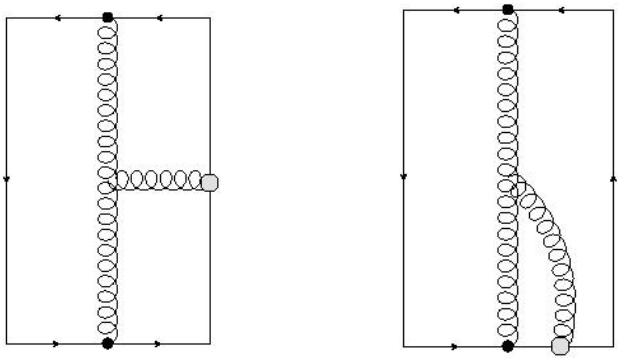

(a) (b)

Figure 2

where a gauge field of Type I from each insertion is connected to a temporal/ spatial axis of the loop through a three-point gluon vertex. Note that all mirrored versions of the diagrams showed above are considered too.
The field on the temporal/ spatial axis arises from the loop expansion discussed in Section 3.1. For the diagram in the left hand side figure it is Equation (36c) that contributes with the first order in the expansion instead of a trivial 1, while for the right hand side figure it is Equation (36b).

Considering the general expression for a three-point gluon vertex in Equation (87) one sees that such a vertex vanishes if the Lorentz indices of the connected fields are either all equal or all different:

$$\begin{aligned} \mu=\nu=\rho \Rightarrow & igf^{abc}\left[\delta_{\mu\mu}\left(k-p\right)_{\mu}+\delta_{\mu\mu}\left(p-q\right)_{\mu}+\delta_{\mu\mu}\left(q-k\right)_{\mu}\right] \\ =&4igf^{abc}\left[k_{\mu}-p_{\mu}+p_{\mu}-q_{\mu}+q_{\mu}-k_{\mu}\right] \\ =&0 \end{aligned} \tag{54a}$$

$$\begin{aligned} \mu\neq\nu\neq\rho \Rightarrow & igf^{abc}\left[0\cdot\left(k-p\right)_{\rho}+0\cdot\left(p-q\right)_{\mu}+0\cdot\left(q-k\right)_{\nu}\right] \\ =&0 \end{aligned} \tag{54b}$$

Therefore, for the right hand side case (see Fig. (2a)), where the field A_0 generated on the temporal axis contributes with $\rho=0$ the other two fields need to have the same Lorentz index which is either $\mu=\nu=i$ or $\mu=\nu=3$.
For the case where a spatial axis field A_3 contributes to the vertex, there are three different possibilities for the remaining Lorentz indices: $\mu=\nu=i$, $\mu=i,\ \nu=3$ or $\mu=3,\ \nu=i$.

Three-point vertex between both insertion contributing with Type I and a temporal axis of the loop

According to the argumentation above I can combine the fields $A_0(t,0,0,\pm r/2)$, $A_3(y)$ and $A_3(y')$ or $A_0(t,0,0,\pm r/2)$, $A_i(y)$ and $A_i(y')$ into a three-point gluon vertex.
For the rest of this section $\pm\vec{z}$ is the short notation for the spatial positions of the loop fields at $(t,\pm\vec{z}) = (t,0,0,\pm r/2)$.
The contour field generator is

$$\begin{aligned} C(A) = ig\Bigg[& \partial_i \mathcal{A}_3(y) \left(\int_{-T/2}^{T/2} \mathrm{d}t \; \mathcal{A}_0(t,\vec{z}) \right) \partial_i \mathcal{A}_3(y') \\ & + \partial_3 \mathcal{A}_i(y) \left(\int_{-T/2}^{T/2} \mathrm{d}t \; \mathcal{A}_0(t,\vec{z}) \right) \partial_3 \mathcal{A}_i(y') \\ & + \left(\partial_i \mathcal{A}_3(y) \partial_i \mathcal{A}_3(y') + \partial_3 \mathcal{A}_i(y) \partial_3 \mathcal{A}_i(y') \right) \int_{T/2}^{-T/2} \mathrm{d}t \; \mathcal{A}_0(t,-\vec{z}) \Bigg] \end{aligned} \tag{55}$$

Depending on whether A_0 is located on the right ($\vec{z}$) or left hand side ($-\vec{z}$) of the loop, the Gell-Mann matrices are sequenced in another order due to the path-ordering of the loop contour fields.
Now, following the short derivation in Section A.2.2 $C(A)$ becomes

$$\frac{ig}{4} \lambda^a \lambda^b \lambda^{a'} \left[\partial_i A_3^a(y) \partial_i A_3^{a'}(y') + \partial_3 A_i^a(y) \partial_3 A_i^{a'}(y') \right] \int_{-T/2}^{T/2} \mathrm{d}t \; A_0^b(t,\vec{z}) \tag{56}$$

With the sets of gluon fields in the upper equation and the general expression for a gluon three-point vertex (see Eq. (87)) the following two vertices can be constructed:

$$igf^{aa'b} \left[\delta_{33}(k_0 - p_0) + \delta_{03}(p_3 - q_3) + \delta_{03}(q_3 - k_3) \right] = igf^{aa'b} \left(k_0 - p_0 \right) \tag{57a}$$

and

$$igf^{aa'b} \left[\delta_{ii}(k_0 - p_0) + \delta_{0i}(p_i - q_i) + \delta_{0i}(q_i - k_i) \right] = igf^{aa'b} \left(k_0 - p_0 \right) \tag{57b}$$

This means that the vertex is independent of the insertions Lorentz indices.
When replacing the gluon fields by propagators and inserting the vertex expression, the diagram becomes

$$\begin{aligned} -\frac{2ig^2}{(2\pi)^8} \int_{-T/2}^{T/2} \mathrm{d}t \int_{k,p,q} & \delta^{(4)}(k+p+q) \frac{k_0 - p_0}{k^2 p^2 q^2} \\ & \times \left(\partial_{y_i} \partial_{y_i'} + \partial_{y_3} \partial_{y_3'} \right) e^{iky} e^{ipy'} e^{iqz} \end{aligned} \tag{58}$$

where I replaced $\lambda^a \lambda^b \lambda^{a'} f^{aa'b} = -\lambda^a \lambda^b \lambda^{a'} f^{ba'a} = -\frac{i}{2} \lambda^a \lambda^a$ and used $\mathrm{Tr}(\lambda^a \lambda^a) = 16$. Moreover, I shortened $(t,\vec{z})$ to z.

The factor $k_0 - p_0$ that results from the three-point vertex makes it more challenging to solve the momentum integrals. Therefore I turn them into derivatives with respect to y_0 and y_0': $k_0 - p_0 \Rightarrow -i\left(\partial_{y_0} - \partial_{y_0'}\right)$.

$$\begin{aligned} &-\frac{2g^2}{(2\pi)^8}\left(\partial_{y_0} - \partial_{y_0'}\right)\left(\partial_{y_i}\partial_{y_i'} + \partial_{y_3}\partial_{y_3'}\right) \\ &\qquad \times \int_{-T/2}^{T/2} \mathrm{d}t \int_{k,p,q} \delta^{(4)}(k+p+q)\frac{1}{k^2p^2q^2} e^{iky} e^{ipy'} e^{iqz} \end{aligned} \tag{59}$$

From here on, the first aim is to solve the three momentum integrations over k, p and q. Therefore, in the following calculations I omit the prefactor $-g^2\lambda^a\lambda^a/8$ as well as the y and y' derivatives and the t integral.
The first momentum integral to solve is q which happens directly when resolving the δ-function and setting $q = -k - p$. This results in

$$\int_{k,p} \frac{1}{(2\pi)^8} \frac{1}{k^2p^2(k+p)^2} e^{iky} e^{ipy'} e^{-i(k+p)z} \tag{60}$$

There is no known convenient way to deal with such momentum integrals containing an exponential factor. Still, there are known mathematical expressions to solve similar integrals with a factor of an arbitrary polynomial of order n $\mathcal{P}_n(k)$ with respect to k. Therefore now an expansion of the exponential functions with respect to k and p is needed. This gives me integrals that can be solved in a relatively easy way. Still, the expansion produces infinite sums that become part of the expression.

First I sort all exponentials in the expression above with respect to the two momenta k and p. This results in

$$e^{iky} e^{ipy'} e^{-i(k+p)z} = e^{ik(y-z)} e^{ip(y'-z)} \tag{61}$$

The two resulting exponentials with respect to k and p can be easily expanded in a Taylor series:

$$e^{ik(y-z)} = \sum_{n=0}^{\infty} \frac{i^n}{n!} \left[k(y-z)\right]^n \tag{62a}$$

$$e^{ip(y'-z)} = \sum_{m=0}^{\infty} \frac{i^m}{m!} \left[p(y'-z)\right]^m \tag{62b}$$

The results of the expansion can be inserted into Equation (60) in order to get an expression with polynomials with respect to k and p:

$$\begin{aligned} &\sum_{n,m=0}^{\infty} \frac{i^{n+m}}{n!m!} \int_{k,p} \frac{1}{(2\pi)^8} \frac{1}{k^2p^2(k+p)^2} \left[k(y-z)\right]^n \left[p(y'-z)\right]^m \\ &= \sum_{n,m=0}^{\infty} \frac{i^{n+m}}{n!m!} \int \frac{\mathrm{d}^4k}{(2\pi)^4} \frac{\left[k(y-z)\right]^n}{k^2} \int \frac{\mathrm{d}^4p}{(2\pi)^4} \frac{\left[p(y'-z)\right]^m}{p^2(k+p)^2} \end{aligned} \tag{63}$$

The p integration was brought in a form where Equation (93) can be applied. It describes how general momentum integrals can be solved through dimensional regularisation (see Section A.1.5).
In the given case the polynomial $\mathcal{P}_m(p)$ is $[p(y'-z)]^m$. Using Equation (93) results in

$$\int \frac{\mathrm{d}^4p}{(2\pi)^4}\frac{[p(y'-z)]^m}{p^2(k+p)^2} = \frac{k^{-2\epsilon}}{(4\pi)^2}\sum_{\sigma=0}^{\infty} G(1,1,m,\sigma)k^{2\sigma}\left\{\frac{1}{\sigma!}\left(\frac{\Box_p}{4}\right)^{\sigma}\mathcal{P}_m(p)\right\}\Bigg|_{p=k} \tag{64a}$$

with

$$G(1,1,m,\sigma) = (4\pi)^{\epsilon}\Gamma(\epsilon-\sigma)B(1+m-\epsilon-\sigma,1-\epsilon+\sigma) \tag{64b}$$

and

$$\begin{aligned} B(1+m-\epsilon-\sigma,1-\epsilon+\sigma) =& \frac{\Gamma(1+m-\epsilon-\sigma)\Gamma(1-\epsilon+\sigma)}{\Gamma(2+m-2\epsilon)} \\ =& \int_0^1 \mathrm{d}t\; t^{\epsilon+\sigma-m}(1-t)^{\epsilon-\sigma} \end{aligned} \tag{64c}$$

Before the k integral can be solved I first have to evaluate $(\Box_p/4)^{\sigma}\mathcal{P}_m(p)$. Note that the d'Alembert operator $\Box_p$ is written in its euclidean representation $\partial^2/\partial p_\mu \partial p_\mu$.
For $(\Box_p/4)^{\sigma}\mathcal{P}_m(p)$ I get

$$\begin{aligned} \left(\frac{\Box_p}{4}\right)^{\sigma}\left[p(y'-z)\right]^m\Bigg|_{p=k} =& \frac{n!}{(n-2\sigma)!}\left(\frac{y'-z}{2}\right)^{2\sigma}\left[p(y'-z)\right]^{m-2\sigma}\Bigg|_{p=k} \\ =& \frac{n!}{(n-2\sigma)!}\left(\frac{y'-z}{2}\right)^{2\sigma}\left[k(y'-z)\right]^{m-2\sigma} \end{aligned} \tag{65}$$

This result is inserted into Equation (64). It now becomes

$$\begin{aligned} &\int \frac{\mathrm{d}^4p}{(2\pi)^4}\frac{[p(y'-z)]^m}{p^2(k+p)^2} \\ =& \frac{k^{-2\epsilon}}{(4\pi)^2}\sum_{\sigma=0}^{\infty} G(1,1,m,\sigma)k^{2\sigma}\frac{n!}{\sigma!(n-2\sigma)!}\left(\frac{y'-z}{2}\right)^{2\sigma}\left[k(y'-z)\right]^{m-2\sigma} \end{aligned} \tag{66}$$

From here on, in order to be able to deal with the k integration, I insert the p integral result into Equation (63) and rearrange the terms.

$$\begin{aligned} &\sum_{n,m=0}^{\infty}\sum_{\sigma=0}^{\infty}\frac{i^{n+m}}{m!\sigma!(n-2\sigma)!}G(1,1,m,\sigma) \\ &\times\frac{1}{(4\pi)^2}\left(\frac{y'-z}{2}\right)^{2\sigma}\int_k \frac{1}{(2\pi)^4}\frac{k^{2(\sigma-\epsilon)}}{k^2}\left[k(y-z)\right]^n\left[k(y'-z)\right]^{m-2\sigma} \end{aligned} \tag{67}$$

Next, the expression above needs to manipulated, so that I can perform the final integration over k by using Equation (93) once more. I rewrite

$$k^{2(\sigma-\epsilon)} = \frac{1}{k^{2(\epsilon-\sigma)}} = \int_q \frac{\delta^{(4)}(q)}{(k+q)^{2(\epsilon-\sigma)}} \tag{68}$$

When inserting that expression into the k integral from Equation (67) I get

$$\int_q \delta^{(4)}(q) \int_k \frac{1}{(2\pi)^4} \frac{[k(y-z)]^n [k(y'-z)]^{m-2\sigma}}{k^2(k+q)^{2(\epsilon-\sigma)}} \tag{69}$$

The integration over the momentum k can now be solved by using Equation (93) with $\alpha = 1$ and $\beta = \epsilon - \sigma$. For that case the polynomial in the nominator is $\mathcal{P}_{n+m-2\sigma}(k) = [k(y-z)]^n [k(y'-z)]^{m-2\sigma}$. Equation (69) becomes

$$\begin{aligned} &\int_q \delta^{(4)}(q) \frac{\left(q^2\right)^{1-\epsilon+\sigma-\delta}}{(4\pi)^2} \\ &\quad \times \sum_{\rho=0}^{\infty} G(1, \epsilon-\sigma, n+m-2\sigma, \rho) q^{2\rho} \left\{ \frac{1}{\rho!} \left(\frac{\Box_k}{4} \right)^{\rho} \mathcal{P}_{n+m-2\sigma}(k) \right\} \Bigg|_{k=q} \end{aligned} \tag{70a}$$

with

$$\begin{aligned} &G(1, \epsilon-\sigma, n+m-2\sigma, \rho) \\ =&(4\pi)^{\delta} \frac{\Gamma(\epsilon+\delta-\sigma-\rho-1)}{\Gamma(1)\Gamma(\epsilon-\sigma)} B(1+n+m-2\sigma-\delta-\rho, 2-\epsilon-\delta+\sigma+\rho) \end{aligned} \tag{70b}$$

and

$$\begin{aligned} &B(1+n+m-2\sigma-\delta-\rho, 2-\epsilon-\delta+\sigma+\rho) \\ =&\frac{\Gamma(1+n+m-2\sigma-\delta-\rho)\Gamma(2-\epsilon-\delta+\sigma+\rho)}{\Gamma(3+n+m-\sigma-\epsilon-2\delta)} \end{aligned} \tag{70c}$$

At this point I can easily get rid of the integration over q with help of the δ-function. All momenta q can then be set to zero what gives the following result:

$$\begin{aligned} &\int_q \delta^{(4)}(q) \frac{\left(q^2\right)^{1-\epsilon+\sigma-\delta}}{(4\pi)^2} \\ &\quad \times \sum_{\rho=0}^{\infty} G(1, \epsilon-\sigma, n+m-2\sigma, \rho) q^{2\rho} \left\{ \frac{1}{\rho!} \left(\frac{\Box_k}{4} \right)^{\rho} \mathcal{P}_{n+m-2\sigma}(k) \right\} \Bigg|_{k=q} \\ =&0 \times \frac{1}{(4\pi)^2} \sum_{\rho=0}^{\infty} G(1, \epsilon-\sigma, n+m-2\sigma, \rho) \left\{ \frac{1}{\rho!} \left(\frac{\Box_k}{4} \right)^{\rho} \mathcal{P}_{n+m-2\sigma}(k) \right\} \Bigg|_{k=0} \\ =&0 \end{aligned} \tag{71}$$

Even though when setting $q = 0$ the term $q^{2\rho}$ in the equation above is undefined for the case $\rho = 0$ the whole expression still vanishes due to the term $\left(q^2\right)^{1-\epsilon+\sigma-\delta}$, where the exponent is always > 0. Therefore when $q = 0$ $\left(q^2\right)^{1-\epsilon+\sigma-\delta} = 0$ for all σ.

This calculation shows that the diagram depicted in Figure (2a) has no contribution to the Π_u hybrid static potential to $\mathcal{O}(g^2)$.

Three-point vertex between both insertions contributing with Type I and a spatial axis of the loop

First, in analogy to the previous section, I figure out what Lorentz indices the gluons generated on the insertions are allowed to have.
The field located on one spatial axis is $A_3(z) = A_3(\pm T/2, 0, 0, s)$ with $s \in (0, \pm r/2]$. The Lorentz index is 3 due to the integration along the z-axis on the spatial loop contours. With the same argumentation as in the previous sections it is clear that there are three possible index combinations: $\mu = i$ and $\nu = 3$, $\mu = 3$ and $\nu = i$ and $\mu = \nu = i$.
For keeping the expression short, for now, I write $C(A)$ for only one section of the spatial axis, namely where $z = (-T/2, 0, 0, s)$ with $s \in (0, r/2]$.

$$\begin{aligned} C(A) = ig\Bigg[&\partial_i \mathcal{A}_3(y) \left(\int_0^{r/2} \mathrm{d}s \; \mathcal{A}_3(z) \right) \partial_3 \mathcal{A}_i(y') \\ &+ \partial_3 \mathcal{A}_i(y) \left(\int_0^{r/2} \mathrm{d}s \; \mathcal{A}_3(z) \right) \partial_i \mathcal{A}_3(y') \\ &+ \partial_3 \mathcal{A}_i(y) \left(\int_0^{r/2} \mathrm{d}s \; \mathcal{A}_3(z) \right) \partial_3 \mathcal{A}_i(y') \Bigg] \end{aligned} \tag{72}$$

First of all, I construct the vertex with matching Lorentz indices for all three cases. The momentum k stays related to the field generated at point y, p to the field at y' while the momentum of the gluon generated at z is q. The three vertices then are

$$\begin{aligned} igf^{aa'b}\left[(k_3 - p_3)\delta_{i3} + (p_3 - q_3)\delta_{i3} + (q_i - k_i)\delta_{33}\right] &= igf^{aa'b}(q_i - k_i) \\ &\to -gf^{aa'b}(\partial_{z_i} - \partial_{y_i}) \end{aligned} \tag{73a}$$

$$\begin{aligned} igf^{aa'b}\left[(k_3 - p_3)\delta_{i3} + (p_i - q_i)\delta_{33} + (q_3 - k_3)\delta_{i3}\right] &= igf^{aa'b}(p_i - q_i) \\ &\to -gf^{aa'b}(\partial_{y'_i} - \partial_{z_i}) \end{aligned} \tag{73b}$$

$$\begin{aligned} igf^{aa'b}\left[(k_3 - p_3)\delta_{ii} + (p_i - q_i)\delta_{i3} + (q_i - k_i)\delta_{i3}\right] &= igf^{aa'b}(k_3 - p_3) \\ &\to -gf^{aa'b}(\partial_{y_3} - \partial_{y'_3}) \end{aligned} \tag{73c}$$

I expressed the momenta from through derivatives by using $k_i \to -i\partial_i$, as it was already done in the previous section.

In the following, I show that mirroring the vertex along the $t = 0$ axis doesn't alter the result. Therefore, it suffices to consider just one spatial axis. For this purpose it is useful to write the diagram that is generated by (72) in terms of propagators and the vertex through derivatives as above. This results in

$$\begin{aligned} &g^2\left[\partial_{y_i}\partial_{y'_3}\left(\partial_{z_i} - \partial_{y_i}\right) + \partial_{y_3}\partial_{y'_i}\left(\partial_{y'_i} - \partial_{z_i}\right) + \partial_{y_3}\partial_{y'_3}\left(\partial_{y_3} - \partial_{y'_3}\right)\right] \\ &\quad \times \int_x \int_0^{r/2} \mathrm{d}s \; \Delta(x - y)\Delta(x - y')\Delta(x - z) \end{aligned} \tag{74}$$

with $\lambda^a\lambda^b\lambda^{a'}f^{aa'b} = -i\lambda^a\lambda^a/2$ and $\mathrm{Tr}(\lambda^a\lambda^a) = 16$ in analogy to the previous section.

Now, I compare this expression to the case where $z' = (T/2, 0, 0, s)$ ($s \in (0, r/2]$) denotes the position of the field on the spatial axis:

$$\begin{aligned} C(A) = ig\Bigg[&\partial_i\mathcal{A}_3(y)\left(\int_{r/2}^{0}\mathrm{d}s\ \mathcal{A}_3(z')\right)\partial_3\mathcal{A}_i(y') \\ &+\partial_3\mathcal{A}_i(y)\left(\int_{r/2}^{0}\mathrm{d}s\ \mathcal{A}_3(z')\right)\partial_i\mathcal{A}_3(y') \\ &+\partial_3\mathcal{A}_i(y)\left(\int_{r/2}^{0}\mathrm{d}s\ \mathcal{A}_3(z')\right)\partial_3\mathcal{A}_i(y')\Bigg] \end{aligned} \tag{75}$$

In order to prove that (72) and (75) result in the same three-point vertex, I write Eq. (75) in a form similar to Eq. (74) and then reform it step by step. First, I get

$$\begin{aligned} &g^2\left[\partial_{y_i}\partial_{y_3'}\left(\partial_{z_i}-\partial_{y_i}\right)+\partial_{y_3}\partial_{y_i'}\left(\partial_{y_i'}-\partial_{z_i}\right)+\partial_{y_3}\partial_{y_3'}\left(\partial_{y_3}-\partial_{y_3'}\right)\right] \\ &\quad\times\int_x\int_{r/2}^{0}\mathrm{d}s\ \Delta(x-y)\Delta(x-y')\Delta(x-z') \end{aligned} \tag{76}$$

Shifting $\Delta(x-z')$ back to $\Delta(x-z)$ requires me to use the relation

$$\begin{aligned} \int_{x_0}\Delta(x-z') &= \int_{x_0}\Delta(x_0-T/2,\vec{x}-\vec{z}) \\ &= \int_{x_0}\Delta(-x_0-T/2,\vec{x}-\vec{z}) \\ &= \int_{x_0}\Delta(x_0+T/2,\vec{x}-\vec{z}) = \int_{x_0}\Delta(x-z) \end{aligned} \tag{77a}$$

where I first performed the substitution $x_0 \to -x_0$ and then used symmetry properties of the propagator. Analogously I can write

$$\int_{x_0}\Delta(x-y) = \int_{x_0}\Delta(x-T/2,\vec{x}-\vec{y}) \tag{77b}$$

and

$$\int_{x_0}\Delta(x-y') = \int_{x_0}\Delta(x+T/2,\vec{x}-\vec{y}') \tag{77c}$$

Then I get

$$
\begin{aligned}
& g^2 \left[\partial_{y_i} \partial_{y_3'} \left(\partial_{z_i} - \partial_{y_i} \right) + \partial_{y_3} \partial_{y_i'} \left(\partial_{y_i'} - \partial_{z_i} \right) + \partial_{y_3} \partial_{y_3'} \left(\partial_{y_3} - \partial_{y_3'} \right) \right] \\
& \quad \times \int_x \int_{r/2}^{0} \mathrm{d}s \; \Delta(x - T/2, \vec{x} - \vec{y}) \Delta(x + T/2, \vec{x} - \vec{y}') \Delta(x - z) \\
\overset{\vec{y} \leftrightarrow \vec{y}'}{=} \; & g^2 \left[\partial_{y_i'} \partial_{y_3} \left(\partial_{z_i} - \partial_{y_i'} \right) + \partial_{y_3'} \partial_{y_i} \left(\partial_{y_i} - \partial_{z_i} \right) + \partial_{y_3'} \partial_{y_3} \left(\partial_{y_3'} - \partial_{y_3} \right) \right] \\
& \quad \times \int_x \int_{r/2}^{0} \mathrm{d}s \; \Delta(x - T/2, \vec{x} - \vec{y}') \Delta(x + T/2, \vec{x} - \vec{y}) \Delta(x - z) \\
= \; & g^2 \left[\partial_{y_3} \partial_{y_i'} \left(\partial_{y_i'} - \partial_{z_i} \right) + \partial_{y_i} \partial_{y_3'} \left(\partial_{z_i} - \partial_{y_i} \right) + \partial_{y_3} \partial_{y_3'} \left(\partial_{y_3} - \partial_{y_3'} \right) \right] \\
& \quad \times \int_x \int_{0}^{r/2} \mathrm{d}s \; \Delta(x - y) \Delta(x - y') \Delta(x - z)
\end{aligned}
\tag{78}
$$

This calculation showed that the upper and lower spatial sections add up, which means that they don't need to be calculated separately.
In the following, I perform the calculation of the diagram that is connected to the spatial axis on the segment between $(-T/2, \vec{0})$ and $(-T/2, 0, 0, r/2)$. The calculation works analogously to the one from the previous section.
In Equation (74) the three-point vertex already had been constructed. Now I additionally write the propagators in coordinate space and express the vertex in terms of a δ-function. Form the last section I know, that the only difference apart from the euclidean vectors is an additional factor of i.

$$
\begin{aligned}
& \frac{g^2}{(2\pi)^8} \left[\partial_{y_i} \partial_{y_3'} \left(\partial_{z_i} - \partial_{y_i} \right) + \partial_{y_3} \partial_{y_i'} \left(\partial_{y_i'} - \partial_{z_i} \right) + \partial_{y_3} \partial_{y_3'} \left(\partial_{y_3} - \partial_{y_3'} \right) \right] \\
& \quad \times \int_0^{r/2} \mathrm{d}s \int_{k,p,q} \delta^{(4)}(k + p + q) \frac{1}{k^2 p^2 q^2} e^{iky} e^{ipy'} e^{iqz}
\end{aligned}
\tag{79}
$$

When comparing this result to Section 7 it is clear that the only differences are the derivatives, that are to be performed at the very end of the calculation and the loop contour integral, which goes along a spatial axis instead of a temporal one as before.
Therefore calculating of the three momentum integrals k, p and q works in full analogy to the previous case.
Since there, solving the integrals lead to a vanishing contribution of the diagram, the same can be concluded for the diagrams discussed in this section.

v1.c1.1

There is only one diagram that can be constructed, when requesting one vertex and one insertion contributing with one order of g. This insertion of Type II generates two gauge fields. The other insertion contributes as Type I with one gauge field. All three fields are connected through a three-point gluon vertex.

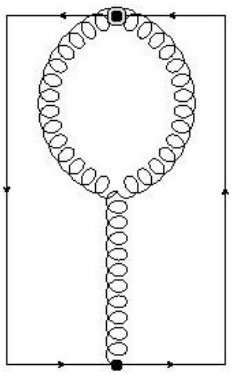

Figure 3

Of course this diagram can be mirrored along the $t = 0$ axis. Then the roles of the insertions would be interchanged.

Again, this diagram does not need to be investigated further due to its r-independence.

v0.c2.0

In this section, I discuss diagrams where two fields, generated on insertions contributing with Type I, are connected to two other fields on the loop contour. Contour fields can be located on six different loop sections. That makes in total 15 possibilities to choose two points on different sections of the loop and additional six possibilities where both fields are located on the same section. Still, due to symmetry considerations, there are only six combinations that need being distinguished:

- One field on a temporal axis and one field on a spatial axis
- Fields on the two opposite temporal axes
- Fields on two opposite spatial axes
- Fields on two adjacent spatial axes
- Two fields on one temporal axis
- Two fields on one spatial axis

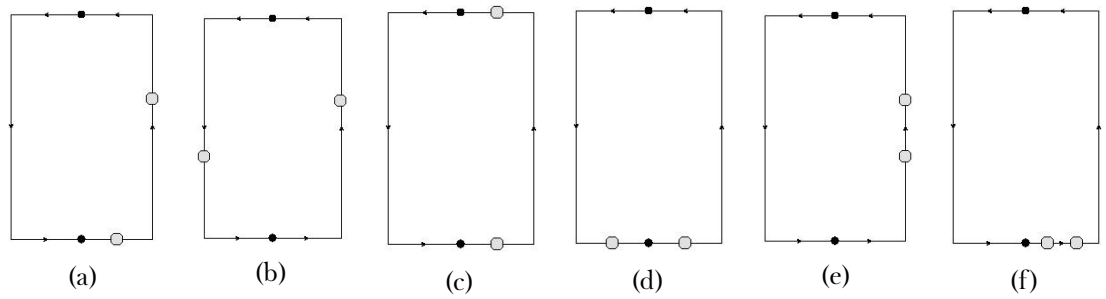

Figure 4

In each case shown Fig. (4) there are two possibilities how to construct propagators. For one it is possible to connect both insertions to one another, as well as both remaining fields. In the other case each insertion field is connected to one of the fields on the Wilson lines.
First, I argue that due to the calculation in Section 4.1 generally only the second of both cases needs to be considered. In the first case the resulting propagator $\Delta(y' - y) = 0$ would always lead to a vanishing diagram.

Now I only need to consider what happens when an insertion is connected to either a field on a temporal or a spatial axis of the loop. Both cases lead to a vanishing contribution. This is due to

1) $A_{i/3}A_0 \rightarrow\ i\Delta_{(i/3)0} = ig_{(i/3)0}\Delta = 0$ which makes propagators connected to a temporal axis become zero trivially.

2) the argumentation in Section 4.4, where I showed that connecting a field on one of the insertions to a field on each of the spatial axes results in a vanishing contribution.

Therefore with the arguments listed above it becomes clear, that all diagrams of type $v0.c2.0$ become zero.

v0.c2.1

Here, the task is to combine four gauge fields from the loop contour into two propagators. Two of the fields are located at one insertion (Type II) and one field on the other insertion (Type I). With this set, the fourth field can only be located on a spatial loop axis. A field from a temporal axis cannot be connected with any of the insertion-fields into a propagator. The resulting diagrams are

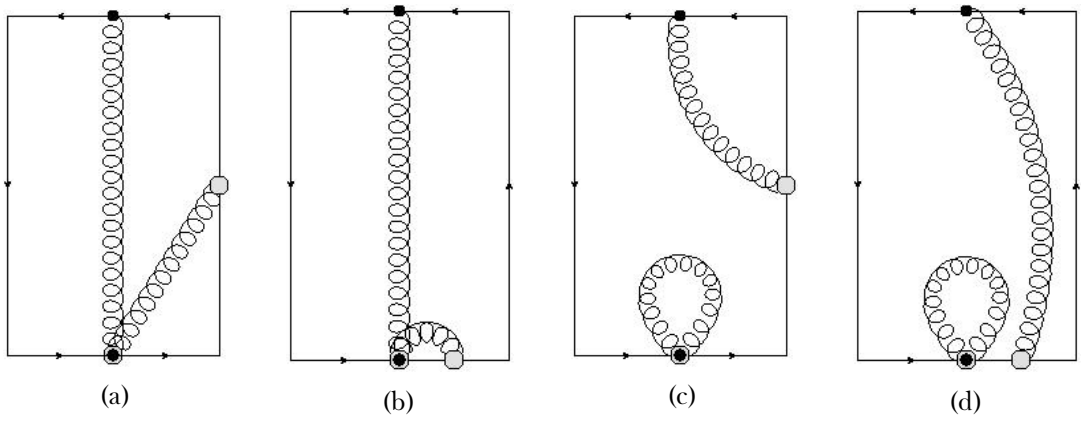

Figure 5

None of them contributes to the second order of g to the Wilson loop expansion. The diagrams in Figs. (5a) and (5b) vanish due to the calculation in Section 4.2 while for Figs. (5c) and (5d) the argument from Section 4.3 applies.

v0.c2.2

There are two possible diagrams to consider.

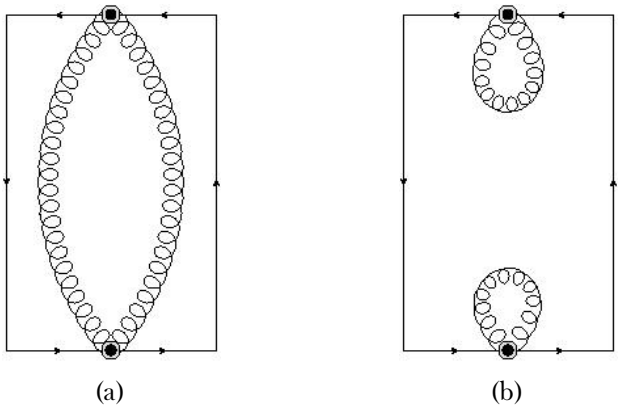

Figure 6

Here again, the diagrams shown are independent of the quark-antiquark distance which means that they are of no importance for the hybrid static potential.

8 The potential to $\mathcal{O}(g^2)$

In the previous sections my focus was the calculation of the Wilson loop expectation value from Equation (32) to the second order in g. I showed that the expression becomes zero to that order.
What remains is the extrapolation onto the hybrid static potential, which is the actual quantity of interest. The formula that relates both quantities is given in Equation (28b). Note that, when using the perturbative approach, there is no straight forward way to make conclusions on the potential from results on the Wilson loop to certain orders. No such general expression has been found jet, what can make according calculations rather complicated.
Luckily, since for the case of the Π_u hybrid the Wilson loop expectation value is zero to the second order in perturbation theory it is rather simple to show that the same applies for the potential. I start with Equation (28b)

$$\begin{aligned} V_{Q\bar{Q}} &= -\lim_{\bar{T}\to\infty} \frac{1}{\bar{T}} \ln\left(\langle W_{\mathcal{C}}\rangle\right) \\ \Rightarrow V_0 + g^2 V_2 + g^4 V_4 + \mathcal{O}(g^6) &= -\lim_{\bar{T}\to\infty} \frac{1}{\bar{T}} \ln\left(W_0 + g^2 W_2 + g^4 W_4 + \mathcal{O}(g^6)\right) \end{aligned} \tag{80}$$

in which I expanded $V_{Q\bar{Q}}$ and $\langle W_{\mathcal{C}}\rangle$ with respect to g. In the next step I focus on the right hand side of the equation. I use $W_0 = W_2 = 0$ and expand the logarithm in terms of a power series.

$$\begin{aligned} \ln\left(W_0 + g^2 W_2 + g^4 W_4 + \mathcal{O}(g^6)\right) &= \ln\left(g^4 W_4 + \mathcal{O}(g^6)\right) \\ &= -\sum_{k=1}^{\infty} \frac{1}{k}\left(1 - g^4 W_4 - \mathcal{O}(g^6)\right)^k \end{aligned} \tag{81}$$

Now I need to argue, why the lowest order contributing to the potential is g^4.
The expression $\left(1 - g^4 W_4 - \mathcal{O}(g^6)\right)^k$ produces terms of at least $\mathcal{O}(g^4)$, except for a 1 adding with each value of k. With the prefactor $1/k$ it is clear to see that this g independent contribution is equivalent to the harmonic series. Therefore the sum in the upper equation can be viewed as

$$\sum_{k=1}^{\infty} \frac{(-1)^k}{k}\left(g^4 W_4 + \mathcal{O}(g^6) - 1\right)^k = \mathcal{O}(g^4) + \sum_{k=1}^{\infty} \frac{1}{k} \tag{82}$$

Note that, of course, the term $\mathcal{O}(g^4)$ on the right hand side of the equation does not contain the same terms as the left hand side but only depicts the orders of g of the terms.
For the consideration of the static potential I can ignore the contribution of the harmonic series since the zero point of the potential can be chosen freely.

Now I finally get

$$\begin{aligned} V_0 + g^2 V_2 + g^4 V_4 + \mathcal{O}(g^6) &= \lim_{\bar{T}\to\infty} \frac{1}{\bar{T}} \mathcal{O}(g^4) \\ &\Rightarrow \underline{\underline{V_0 = V_2 = 0}} \end{aligned} \tag{83}$$

which shows that the Π_u hybrid static potential is zero up to the second order in perturbation theory.

9 Conclusion

In Sections 5, 6 and 7 I have constructed all diagrams that are involved in the zeroth to second order of the Π_u hybrid static potential correlation function and proved them to be zero.

Most of the diagrams were rather easy to calculate through usage of the rules for simple propagators on the Wilson loop, which I wrote down in Section 4. These rules led to vanishing contributions for diagrams of kind v0.c2.0 and v0.c2.1.
There were also some cases I could ignore completely, namely v2.c0.0, v1.c1.1 and v0.c2.2 diagrams. Due to their r-independence their contribution to the potential is only a constant of no particular interest.
The interesting diagrams were of type v1.c1.0. They involve a free three-point gluon vertex between both insertions and one loop axis. Due to the fixed positions of the insertions, the arising integrals contained exponential factors. They impeded the calculation, making it impossible to solve the integrals as it was done in [21] for ordinary Wilson loops that lack an insertion.
Instead I approached the problem through writing the exponentials via its Taylor series. Only then it became possible to apply the formula introduced in A.1.5 which solves momentum integrals containing arbitrary polynomials in dimensional regularisation in terms of a power series. In total, I applied Equation (93) two times. The important step, for showing that the diagram becomes zero, was to construct an additional integral containing a δ-function (see Eq. (68)). The δ-function then was able to make the diagram vanish.

With that results for the zeroth, first and second order in the expansion of the Wilson loop, I was able to draw conclusions on the hybrid static potential to $\mathcal{O}(g^2)$. This has been done in Section 8. There I showed, that the Π_u hybrid static potential becomes zero to the second order in perturbation theory. That result is in agreement with the statement that had been made in [1].

10 Outlook

In general, the perturbative approach to hybrid static potentials proofs to be rather lengthy due to the amount of diagrams that needs to be calculated. The second order in perturbation theory, which I was dealing with in this work, is still manageable. In Section 6 I showed that all odd orders of g become zero trivially. This makes the next order of interest $\mathcal{O}(g^4)$, where the number of diagrams rises considerably.
In the following table I give an overview over all diagrams of order g^4. The notation is analogous to the diagrams of order g^2.

	$n_c = 2$			$n_c = 1$		$n_c = 0$
	$n_i = 2$ $n_w = 0$	$n_i = 1$ $n_w = 1$	$n_i = 0$ $n_w = 1$	$n_i = 1$ $n_w = 0$	$n_i = 0$ $n_w = 1$	$n_i = 0$ $n_w = 0$
$n_v = 2$	v2.c2.2	v2.c2.1	v2.c2.0			
$n_v = 3$				v3.c1.1	v3.c1.0	
$n_v = 4$						v4.c0.0
	$n_c = 4$			$n_c = 3$		
	$n_i = 2$ $n_w = 2$	$n_i = 1$ $n_w = 3$	$n_i = 0$ $n_w = 4$	$n_i = 2$ $n_w = 1$	$n_i = 1$ $n_w = 2$	$n_i = 0$ $n_w = 3$
$n_v = 0$	v0.c4.2	v0.c4.1	v0.c4.0			
$n_v = 1$				v1.c3.2	v1.c3.1	v1.c3.0

Table 3: The designation of diagrams is analogous to how it was done for $\mathcal{O}(g^2)$ in Table (2). Here the total order of the diagrams is $\mathcal{O}(g^4)$. Therefore the sum of the first to numbers in the description of each kind is 4 instead of 2, as it was in Table (2).

Of course, for each kind listed in the table there are several subdiagrams that need to be considered separately.
Apart from the amount of calculation needed to be performed in higher orders, they also become increasingly complicated. As could be seen in the calculation of the v1.c1.0 diagrams, the presence of insertions make standard approaches to the diagrams impossible. Therefore, new calculation methods for that type of integrals would be needed to make the investigation of higher orders feasible.

On the other hand, based on the calculations performed in this work, it should be easily possible to proof another statement from [1], namely that the next excited hybrid system, Σ_u^- should equal the octet potential V_O up the order g^2. The only difference between Π_u and Σ_u^- static potentials are the Lorentz indices contained in their insertions, which don't have any influence on most of the calculation. As can be looked up in Table (1) the Σ_u^- insertion is $H^{AB} = (\hat{e}_3)_i B_i^{AB} = B_3^{AB} = -\frac{1}{2}\epsilon_{3jk}\mathcal{F}_{jk}^{AB}$. This means that all calculations considering the Σ_u^- hybrid should work in analogy to the ones performed in this work.
Moreover, it should be possible to perform analogous calculations for even higher hybrid static potentials. Such data up to the second order in perturbation theory could allow drawing conclusions on the accuracy of this approach when comparing the results to lattice data.

A Appendix

A.1 Formulas

A.1.1 Relations of Gell-Mann matrices and structure constants

In the following I sum up some useful relations of Gell-Mann matrices and structure constants, that are used in the course of my calculations:

$$\lambda^a \lambda^b = \frac{1}{2}\left[\frac{1}{3}\delta^{ab}\mathbb{1} + \left(d^{abc} + if^{abc}\right)\lambda^c\right] \tag{84}$$

$$\mathrm{Tr}\left[\lambda^a \lambda^b\right] = 2\delta^{ab} \quad \Rightarrow \quad \mathrm{Tr}\left[\lambda^a \lambda^a\right] = 16 \tag{85}$$

$$f^{abc} f^{a'bc} = 3\delta^{aa'} \tag{86}$$

The relations above are taken from [22].

A.1.2 Euclidean Feynman rules

3-gluon vertex:

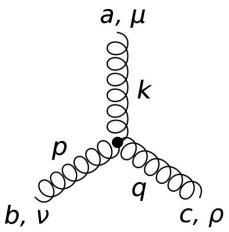

$$igf^{abc}\left[\delta_{\mu\nu}\left(k-p\right)_\rho + \delta_{\nu\rho}\left(p-q\right)_\mu + \delta_{\mu\rho}\left(q-k\right)_\nu\right] \tag{87}$$

4-gluon vertex:

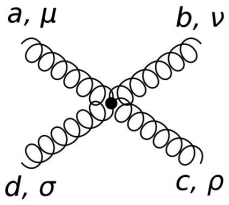

$$\begin{aligned} -g^2\Big[&f^{abe}f^{cde}\left(\delta_{\mu\rho}\delta_{\nu\sigma} - \delta_{\mu\sigma}\delta_{\nu\rho}\right) + f^{ace}f^{bde}\left(\delta_{\mu\nu}\delta_{\rho\sigma} - \delta_{\mu\sigma}\delta_{\nu\rho}\right) \\ &+ f^{ade}f^{bce}\left(\delta_{\mu\nu}\delta_{\rho\sigma} - \delta_{\mu\rho}\delta_{\nu\sigma}\right)\Big] \end{aligned} \tag{88}$$

The Feynman rules in euclidean space-time are taken from [23].

A.1.3 Grassmann integrals

One can derive the solution of the following integral over Grassmann variables as

$$\begin{aligned} &\int D(\bar{\Psi}\Psi)\Psi_{i_1}...\Psi_{i_l}\bar{\Psi}_{i'_1}...\bar{\Psi}_{i'_l}\exp\left[-\sum_{ij}\bar{\Psi}_i K_{ij}\Psi_j\right] \\ =&\xi_l(\det K)\sum_P(-1)^{\sigma_P}K^{-1}_{i_1 i'_{P_1}}...K^{-1}_{i_l i'_{Pl}} \end{aligned} \tag{89}$$

where K_{ij} is a matrix of a fitting dimension, $\xi_l = (-1)^{l(l-1)/2}$ and P denotes all the possible permutations of indices to sum over.

A.1.4 Fourier transformation of euclidean gluon propagator

The general formula

$$\int \frac{d^D k}{(2\pi)^D} \frac{e^{ikx}}{(k^2)^{D/2-\alpha}} = \frac{\Gamma(\alpha)}{(2\pi)^{D/2}\Gamma(D/2-\alpha)} \frac{1}{x^{2\alpha}} \tag{90}$$

taken from [24] helps solving the integral

$$\int \frac{d^4 k}{(2\pi)^4} \frac{e^{ikx}}{k^2} \tag{91}$$

which is part of the euclidean gluon propagator in Feynman gauge. With $D = 4$ and $\alpha = 1$ Equation (90) leads to the following result:

$$\int \frac{d^4 k}{(2\pi)^4} \frac{e^{ikx}}{k^2} = \frac{1}{(2\pi)^2} \frac{1}{x^2} \tag{92}$$

A.1.5 General result for momentum integrals in dimensional regularization

Momentum integrals containing arbitrary polynomials of order n with respect to the integration variable (a momentum four-vector) can be solved in dimensional regularization through a general integration formula derived in [24]:

$$\begin{aligned} &\int \frac{\mathrm{d}^D p}{(2\pi)^D} \frac{\mathcal{P}_n(p)}{p^{2\alpha}(k+p)^{2\beta}} \\ &\quad = \frac{\left(k^2\right)^{2-\alpha-\beta-\epsilon}}{(4\pi)^2} \sum_{\sigma=0}^{\infty} G(\alpha,\beta,n,\sigma) k^{2\sigma} \left\{ \frac{1}{\sigma!} \left(\frac{\Box_p}{4} \right)^{\sigma} \mathcal{P}_n(p) \right\} \Bigg|_{p=k} \end{aligned} \tag{93}$$

Here $\mathcal{P}_n(p)$ denotes the polynomial. In general it can also have a dependence on other momenta. α and β are of the form $n + \epsilon$, n being an integer and ϵ an infinitesimal parameter accounting for dimensional regularisation.
The function G is defined as

$$G(\alpha,\beta,n,\sigma) = (4\pi)^{\epsilon} \frac{\Gamma(\alpha+\beta-2+\epsilon-\sigma)}{\Gamma(\alpha)\Gamma(\beta)} B(2-\alpha+n-\epsilon-\sigma, 2-\beta-\epsilon+\sigma) \tag{94a}$$

where $B(x, y)$ is the Euler beta function, which is defined as

$$B(x,y) = \frac{\Gamma(x)\Gamma(y)}{\Gamma(x+y)} = \int_0^1 \mathrm{d}t\, t^{1-x}(1-t)^{1-y} \tag{94b}$$

A.2 Calculations

A.2.1 Integration of static (anti-)quark fields from the meson correlation function

The starting point of the evaluation of the static (anti-)quark contribution to the correlation function of a static $Q\bar{Q}$ system is Equation (24a). The quark field integrals are

$$\int \mathrm{D}\Psi\mathrm{D}\bar{\Psi}\ \bar{\Psi}^{B'}_{\beta'}(y')\Psi^{A'}_{\alpha'}(x')\bar{\Psi}^{A}_{\alpha}(x)\Psi^{B}_{\beta}(y)\ e^{iS_Q} \tag{95a}$$

in the nominator and

$$\int \mathrm{D}\Psi\mathrm{D}\bar{\Psi}\ e^{iS_Q} \tag{95b}$$

in the denominator.
In both cases Equation (89) can be used in order to find results for the Grassmann-valued integrals. According to the general formula the two integrals become

$$\begin{aligned}(-1)^{2(2-1)/2}&\det K\\ &\times\left[K^{A'B'}_{\alpha'\beta'}(x',y')^{-1}K^{BA}_{\beta\alpha}(y,x)^{-1}-K^{A'A}_{\alpha'\alpha}(x',x)^{-1}K^{BB'}_{\beta\beta'}(y,y')^{-1}\right]\\ =\det K&\left[K^{A'A}_{\alpha'\alpha}(x',x)^{-1}K^{bb'}_{\beta\beta'}(y,y')^{-1}-K^{A'B'}_{\alpha'\beta'}(x',y')^{-1}K^{BA}_{\beta\alpha}(y,x)^{-1}\right]\end{aligned} \tag{96a}$$

and

$$\det K \tag{96b}$$

Writing the integration results in their original form as a fraction the determinant can be cancelled:

$$\begin{aligned}&\frac{\int \mathrm{D}\Psi\mathrm{D}\bar{\Psi}\ \bar{\Psi}^{B'}_{\beta'}(y')\Psi^{A'}_{\alpha'}(x')\bar{\Psi}^{A}_{\alpha}(x)\Psi^{B}_{\beta}(y)\ e^{iS_Q}}{\int \mathrm{D}\Psi\mathrm{D}\bar{\Psi}\ e^{iS_Q}}\\ =&K^{A'A}_{\alpha'\alpha}(x',x)^{-1}K^{BB'}_{\beta\beta'}(y,y')^{-1}-K^{A'B'}_{\alpha'\beta'}(x',y')^{-1}K^{BA}_{\beta\alpha}(y,x)^{-1}\end{aligned} \tag{97}$$

In the current case, where the Grassmann-valued integral is a path-integral for Dirac fields the matrix K can be identified as

$$K^{A'A}_{\alpha'\alpha}(x',x)=-i\left[i\gamma_\mu D^\mu(x')-M\right]_{\alpha'\alpha}\delta^{AA'}\delta^{(4)}(x'-x) \tag{98}$$

This knowledge makes it possible to determine its inverse K^{-1} as

$$K^{A'A}_{\alpha'\alpha}(x',x)^{-1}=S_{\alpha'\alpha}(x'-x)\ \mathcal{P}\left\{\exp\left[ig\int_{x_0}^{x'_0}\mathrm{d}t\ \mathcal{A}^0(t,\vec{x}')\right]\right\}^{A'A} \tag{99a}$$

with

$$S_{\alpha\beta}(x'-x) = \delta^{(3)}(\vec{x}'-\vec{x}) \left\{ \Theta(x'_0-x_0) \left[\frac{1+\gamma_0}{2}\right]_{\alpha'\alpha} e^{-iM(x'_0-x_0)} + \Theta(x_0-x'_0) \left[\frac{1-\gamma_0}{2}\right]_{\alpha'\alpha} e^{iM(x'_0-x_0)} \right\} \tag{99b}$$

It can be seen that the exponential contribution to K^{-1} is actually nothing but a temporal Wilson line:

$$U^{A'A}(x',x) = \mathcal{P}\left\{ \exp\left[-ig \int_{x_0}^{x'_0} \mathrm{d}t\, \mathcal{A}^0(t,\vec{x}') \right] \right\}^{A'A} \tag{100}$$

The resulting expression for K^{-1} can be inserted into the static (anti-)quark contribution (see Eq. (97)) to the hybrids correlation function.
The contribution of $K(x',y')^{-1}K(y,x)^{-1}$ becomes zero immediately due to the δ-functions $\delta^{(3)}(\vec{x}'-\vec{y}')\delta^{(3)}(\vec{y}-\vec{x})$. They do not contribute because infinitely heavy quarks are frozen on their positions which in the current case are $\vec{x}=\vec{x}'=\vec{r}/2 \neq -\vec{r}/2 = \vec{y}=\vec{y}'$.
Equation (97) becomes

$$\begin{aligned} & K^{A'A}_{\alpha'\alpha}(x',x)^{-1} K^{BB'}_{\beta\beta'}(y,y')^{-1} \\ =& \delta^{(3)}(\vec{x}'-\vec{x})\, \delta^{(3)}(\vec{y}-\vec{y}') \left[\frac{1+\gamma_0}{2}\right]_{\alpha'\alpha} \left[\frac{1-\gamma_0}{2}\right]_{\beta\beta'} e^{-2iMT} \\ & \times \mathcal{P}\left\{ U^{A'A}(x',x) U^{BB'}(y,y') \right\} \end{aligned} \tag{101}$$

In order to get that result the Θ-functions had already been evaluated as $\Theta(x'_0-x_0) = \Theta(y'_0-y_0) = \Theta(T) = 1$ and $\Theta(x_0-x'_0) = \Theta(y_0-y'_0) = \Theta(-T) = 0$.
Before inserting this result into the correlation function in Equation (24a) it is useful to first combine the contributions of the temporal Wilson lines that result from the static quark integrals with the Wilson lines $U(x,y)$ and $U(y',x')$ from the correlation function:

$$U^{B'A'}(y',x')U^{A'A}(x',x)U^{AB}(x,y)U^{BB'}(y,y') = \exp\left[-ig \oint_{\mathcal{C}} \mathrm{d}z_\mu \mathcal{A}^\mu(z) \right] \tag{102}$$

Then the final path-integral result for the correlation function becomes

$$\begin{aligned} \langle \Phi(T)|\Phi(0)\rangle = & -\delta^{(3)}\left(\vec{x}-\vec{x}'\right) \delta^{(3)}\left(\vec{y}-\vec{y}'\right) \\ & \times \mathrm{Tr}\left[(P_+)_{\alpha\alpha'} (P_-)_{\beta\beta'} \frac{\mathcal{P}}{Z'} \int D\bar{\eta}D\eta DA\; e^{-ig\oint_{\mathcal{C}} \mathrm{d}z_\mu \mathcal{A}^\mu(z)} e^{-2iMT} e^{iS_G} \right] \end{aligned} \tag{103a}$$

with

$$Z' = \int D\bar{\eta}D\eta DA\; e^{iS_G} \tag{103b}$$

and

$$P_\pm = \frac{1\pm\gamma_0}{2} \tag{103c}$$

A.2.2 Derivation of three-point vertex contour field generator

Below you see the part of the contour field generator of the three-point gluon vertex in Section 7 with Lorentz indices $\mu = \nu = 3$ and $\rho = 0$.

$$ig\left[\partial_i\mathcal{A}_3(z)\left(\int_{-T/2}^{T/2}\mathrm{d}t\;\mathcal{A}_0(t,\vec{y})\right)\partial_i\mathcal{A}_3(z') + \partial_i\mathcal{A}_3(z)\partial_i\mathcal{A}_3(z')\int_{T/2}^{-T/2}\mathrm{d}t\;\mathcal{A}_0(t,-\vec{y})\right] \tag{104}$$

It is possible to show that the two integrals over the temporal loop axes can be merged into one. For this I make use of the negative parity of gluons: $\mathcal{A}(x_0,\vec{x}) \to -\mathcal{A}(x_0,-\vec{x})$. Then the second set of gluon fields from Equation (104) becomes

$$\begin{aligned}
&\mathcal{A}_3(z)\mathcal{A}_3(z')\mathcal{A}_0(t,-\vec{y}) \\
=&-\mathcal{A}_3(z)\mathcal{A}_0(t,\vec{y})\mathcal{A}_3(z') \\
=&-\frac{\lambda^a\lambda^b\lambda^{a'}}{8}A_3^a(z)A_0^b(t,\vec{y})A_3^{a'}(z')
\end{aligned} \tag{105}$$

When using this identity and interchanging the boundaries of the second integral Equation (104) becomes

$$\frac{ig}{4}\lambda^a\lambda^b\lambda^{a'}\partial_iA_3^a(z)\partial_iA_3^{a'}(z')\int_{-T/2}^{T/2}\mathrm{d}t\;A_0^b(t,\vec{y}) \tag{106}$$

This calculation works analogously for the Lorentz indices $\mu = \nu = i$ and $\rho = 0$.

References

[1] G. S. Bali. QCD potentiology. In *4th International Conference on Quark Confinement and the Hadron Spectrum*, 7 2000.

[2] Richard F. Lebed, Ryan E. Mitchell, and Eric S. Swanson. Heavy-quark qcd exotica. *Progress in Particle and Nuclear Physics*, 93:143–194, Mar 2017.

[3] Eric Swanson. Xyz states: Theory overview. 1735:020013, 05 2016.

[4] C.A. Meyer and E.S. Swanson. Hybrid mesons. *Progress in Particle and Nuclear Physics*, 82:21–58, May 2015.

[5] Stephen Lars Olsen, Tomasz Skwarnicki, and Daria Zieminska. Nonstandard heavy mesons and baryons: Experimental evidence. *Reviews of Modern Physics*, 90(1), Feb 2018.

[6] Nora Brambilla, Simon Eidelman, Christoph Hanhart, Alexey Nefediev, Cheng-Ping Shen, Christopher E. Thomas, Antonio Vairo, and Chang-Zheng Yuan. The xyz states: Experimental and theoretical status and perspectives. *Physics Reports*, 873:1–154, Aug 2020.

[7] Michelle Weber. The bottomonium spectrum from the static potential. Master's thesis, Institut für Theoretische Physik, Goethe Universität Frankfurt am Main, March 2017.

[8] York Schröder. The static potential in qcd to two loops. *Physics Letters B*, 447(3-4):321–326, Feb 1999.

[9] Markus Peter. The static potential in qcd — a full two-loop calculation. *Nuclear Physics B*, 501(2):471–494, Sep 1997.

[10] Markus Peter. Static quark-antiquark potential in qcd to three loops. *Physical Review Letters*, 78(4):602–605, Jan 1997.

[11] Owe Philipsen. *Quantenfeldtheorie und das Standardmodell der Teilchenphysik: Eine Einführung*. 01 2018.

[12] Michael E. Peskin and Daniel V. Schroeder. *An Introduction to quantum field theory*. Addison-Wesley, Reading, USA, 1995.

[13] Heinz J Rothe. *Lattice gauge theories: an introduction*, volume 74. World Scientific Publishing Company, 2005.

[14] Krusche Amsler, DeGrand. Quark model. September 2008.

[15] Y. M. Yao et al. [Particle Data Group Collaboration]. Review of particle physics. *Journal of Physics G: Nuclear and Particle Physics*, 33(1):1232, July 2006.

[16] C. A. Meyer and Y. Van Haarlem. Status of exotic-quantum-number mesons. *Physical Review C*, 82(2), Aug 2010.

[17] Matthias Berwein, Nora Brambilla, Jaume Tarrús Castellà, and Antonio Vairo. Quarkonium hybrids with nonrelativistic effective field theories. *Physical Review D*, 92(11), Dec 2015.

[18] E. M. Lifshitz L. D. Landau. *Quantum Mechanics: Non-Relativistic Theory*, volume 3. Pergamon Press, 1977.

[19] Gunnar S. Bali. Qcd forces and heavy quark bound states. *Physics Reports*, 343(1-2):1–136, Mar 2001.

[20] Nora Brambilla, Antonio Pineda, Joan Soto, and Antonio Vairo. Potential nrqcd: an effective theory for heavy quarkonium. *Nuclear Physics B*, 566(1-2):275–310, Jan 2000.

[21] York Schroder. *The Static potential in QCD*. PhD thesis, Hamburg U., 1999.

[22] Howard E. Haber. Useful relations among the generators in the defining and adjoint representations of su(n). *SciPost Physics Lecture Notes*, January 2021.

[23] Pierre Ramond. *Field Theory: A Modern Primer*. Front.Phys. 51 (1981) 1-397, Front.Phys. 74 (1989) 1-329, 1981.

[24] K. G. Chetyrkin and F. V. Tkachov. Integration by Parts: The Algorithm to Calculate beta Functions in 4 Loops. *Nucl. Phys. B*, 192:159–204, 1981.